


## RESEARCH ARTICLE

# Task-related changes in degree centrality and local coherence of the posterior cingulate cortex after major cardiac surgery in older adults

Jeffrey N. Browndyke<sup>1,2,3\*</sup>  | Miles Berger<sup>4\*</sup> | Patrick J. Smith<sup>5</sup> |  
 Todd B. Harshbarger<sup>3,6</sup> | Zachary A. Monge<sup>7</sup> | Viral Panchal<sup>8</sup> | Tiffany L. Bisanar<sup>8</sup> |  
 Donald D. Glower<sup>9</sup> | John H. Alexander<sup>10</sup> | Roberto Cabeza<sup>2,3,7</sup> |  
 Kathleen Welsh-Bohmer<sup>1,11</sup> | Mark F. Newman<sup>8</sup> |  
 Joseph P. Mathew,<sup>8</sup> for the Duke Neurologic Outcomes Research Group (NORG)<sup>†</sup>

<sup>1</sup>Geriatric Behavioral Health Division, Department of Psychiatry & Behavioral Sciences, Duke University Health System, Durham, North Carolina

<sup>2</sup>Duke Institute for Brain Sciences, Duke University, Durham, North Carolina

<sup>3</sup>Duke Brain Imaging and Analysis Center, Duke University, Durham, North Carolina

<sup>4</sup>Division of Neuroanesthesiology, Department of Anesthesiology, Duke University Medical Center, Durham, North Carolina

<sup>5</sup>Behavioral Medicine Division, Department of Psychiatry & Behavioral Sciences, Duke University Medical Center, Durham, North Carolina

<sup>6</sup>Department of Radiology, Duke University Medical Center, Durham, North Carolina

<sup>7</sup>Center for Cognitive Neuroscience, Duke University, Durham, North Carolina

<sup>8</sup>Department of Anesthesiology, Duke University Medical Center, Durham, North Carolina

<sup>9</sup>Cardiovascular & Thoracic Division, Department of Surgery, Duke University Medical Center, Durham, North Carolina

<sup>10</sup>Duke Clinical Research Institute, Duke University Medical Center, Durham, North Carolina

<sup>11</sup>Department of Neurology, Duke University Medical Center, Durham, North Carolina

## Correspondence

Jeffrey N. Browndyke, PhD, Geriatric Behavioral Health Division, Department of Psychiatry & Behavioral Sciences, Duke University Medical Center, 2200 West Main Street, Suite A-200, Durham, NC 27705, USA.  
 Email: j.browndyke@duke.edu

## Funding information

Research supported, in part, by the National Heart, Lung, and Blood Institute grants HL109971 (JNB & JPM), HL096978 (JPM) and HL108280 (JPM); and National Institute on Aging grants AG042599 (JNB) and AG050918 (MB).

## Abstract

**Objectives:** Older adults often display postoperative cognitive decline (POCD) after surgery, yet it is unclear to what extent functional connectivity (FC) alterations may underlie these deficits. We examined for postoperative voxel-wise FC changes in response to increased working memory load demands in cardiac surgery patients and nonsurgical controls.

**Experimental design:** Older cardiac surgery patients ( $n = 25$ ) completed a verbal N-back working memory task during MRI scanning and cognitive testing before and 6 weeks after surgery; nonsurgical controls with cardiac disease ( $n = 26$ ) underwent these assessments at identical time intervals. We measured postoperative changes in degree centrality, the number of edges attached to a brain node, and local coherence, the temporal homogeneity of regional functional correlations, using voxel-wise graph theory-based FC metrics. Group  $\times$  time differences were evaluated in these FC metrics associated with increased N-back working memory load (2-back > 1-back), using a two-stage partitioned variance, mixed ANCOVA.

**Principal observations:** Cardiac surgery patients demonstrated postoperative working memory load-related degree centrality increases in the left dorsal posterior cingulate cortex (dPCC;

\*Jeffrey N. Browndyke and Miles Berger contributed equally to this study.

<sup>†</sup>NORG members are listed in the Appendix.

$p < .001$ , cluster  $p\text{-FWE} < .05$ ). The dPCC also showed a postoperative increase in working memory load-associated local coherence ( $p < .001$ , cluster  $p\text{-FWE} < .05$ ). dPCC degree centrality and local coherence increases were inversely associated with global cognitive change in surgery patients ( $p < .01$ ), but not in controls.

**Conclusions:** Cardiac surgery patients showed postoperative increases in working memory load-associated degree centrality and local coherence of the dPCC that were inversely associated with postoperative global cognitive outcomes and independent of perioperative cerebrovascular damage.

#### KEYWORDS

brain, magnetic resonance imaging, functional neuroimaging, cognitive dysfunction, thoracic surgery, anesthesia, gyrus cingula, neuropsychological tests, memory, short-term, attention

## 1 | INTRODUCTION

Although major surgery is often viewed as a transient physiologic perturbation, increasing evidence suggests that many patients may experience sustained cognitive deficits afterwards. These postoperative cognitive changes occur more frequently in older adults and have been studied extensively after cardiac surgery (Newman et al., 2001a, 2001b). Up to 40% of older adults may experience postoperative cognitive dysfunction (POCD), a syndrome describing cognitive deficits (measured by pre- and postoperative neuropsychological tests) that lasts for weeks to months postsurgery (Berger et al., 2015; Canet et al., 2003; Coburn, Fahlenkamp, Zoremba, & Schaelte, 2010; Gao et al., 2005; Ida and Kawaguchi, 2014; Johnson et al., 2002; Kotekar, Kuruvilla, & Murthy, 2014; Lombard and Mathew, 2010; Monk et al., 2008; Newfield, 2009; Newman, Stygall, Hirani, Shaefi, & Maze, 2007; Ramaiiah and Lam, 2009; Rasmussen, 2006; Sauer, Kalkman, & van Dijk, 2009; van Dijk, Dieleman, & Hijman, 2007). POCD has also been associated with longer term cognitive decline, decreased quality of life, and increased mortality risk (Monk et al., 2008).

Patients with POCD following cardiac and noncardiac surgeries frequently display attention and executive deficits on cognitive testing (Price, Garvan, & Monk, 2008; Raja, Blumenthal, & Doraiswamy, 2004), and often complain of difficulty completing tasks that require concerted cognitive effort or high working memory demands (Phillips-Bute et al., 2006). Working memory load refers to holding increasingly more information “online” while manipulating aspects of that information (Stanley, Dagenbach, Lyday, Burdette, & Laurienti, 2014). Only one prior study has directly examined working memory-related functional imaging changes after cardiac surgery. Abu-Omar et al. (2006) found significant prefrontal cortex fMRI signal intensity decreases during a working memory task in patients undergoing cardiac surgery with cardiopulmonary bypass relative to those undergoing cardiac surgery without cardiopulmonary bypass (i.e., “off-pump”). In the on-pump patients, postoperative changes in prefrontal cortex fMRI activity during very high working memory load demand were inversely associated with intraoperative emboli number as detected by transcranial Doppler ultrasound; suggesting that the lingering effects of intraoperative

embolic load might cause postoperative alterations in prefrontal cortex activation during high working memory load tasks.

The Abu-Omar et al.’s (2006) study appears to support a possible embolic mechanism for cardiac surgery-related POCD, as perioperative cerebral embolization risk from particulate and gaseous materials is increased by cardiopulmonary bypass cross-clamping, vessel cannulation, and reperfusion procedures (Motallebzadeh, Bland, Markus, Kaski, & Jahangiri, 2007). It is clear that perioperative cerebral particulate and gaseous emboli are a salient concern during cardiac surgery (Brown, Moody, Challa, Stump, & Hammon, 2000; Lynch and Riley, 2008; Notzold, Khattab, & Eggers, 2006; Zanatta et al., 2013). However, evidence for an embolic POCD etiology has been mixed (Kruis, Vlasveld, & Van Dijk, 2010) with many surgical outcome trials finding no significant or lingering associations between perioperative emboli and cognition (Browndyke et al., 2002; Cook et al., 2007; Liu et al., 2009; Rodriguez, Rubens, Wozny, & Nathan, 2010; Scott et al., 2014). The mixed evidence for an embolic etiology underlying POCD may be due, in part, to the inherently idiosyncratic emboli volumes and heterogeneous spatial distribution of perioperative particulate and gaseous embolic-related cerebrovascular damage and ischemia (Patel, Minhas, & Chung, 2015). Additionally, there are known peri- and postoperative neuroinflammatory systemic changes that may be related to embolization-associated ischemia and have broader, distributed effects on the cortex and cerebral functioning (Di Napoli and Shah, 2011; Maddahi and Edvinsson, 2010).

Neuroinflammation has been posited as a possible etiological mechanism for POCD (Vacas, Degos, Feng, & Maze, 2013) and postoperative delirium (Cerejeira, Firmino, Vaz-Serra, & Mukaetova-Ladinska, 2010; Cortese and Burger, 2017). Surgery, independent of type, causes a systemic immune response which, in turn, triggers the broad release of proinflammatory cytokines and microglia activation in the central nervous system that may be deleterious to postoperative cognition and increase delirium risk in older patients (Berger, Burke, Eckenhoff, & Mathew, 2014). Biomarkers of CNS inflammation have been found in the CSF and plasma of older noncardiac surgery patients (Hirsch et al., 2016), and biomarkers of direct brain cellular injury (e.g., plasma glial fibrillary acid) following orthopedic surgery that appear to be inversely

associated with postsurgical cognitive outcomes (Rappold et al., 2016). Neuroinflammation following cardiac surgery has been demonstrated in rodent models to be wide spread throughout the brain (Hovens, van Leeuwen, Mariani, Kraneveld, & Schoemaker, 2016), and experimentally induced systemic neuroinflammation has been demonstrated in humans to affect brain functional connectivity in large-scale networks associated with working memory performance (Labrenz et al., 2016). Thus, emboli-related cerebrovascular damage and neuroinflammation are two, potentially nonmutually exclusive, etiologies that may be working in concert to produce the postoperative working memory and executive deficits so often manifest in older patient surgery samples.

Working memory task performance has been associated with multiple large-scale brain networks, including the frontoparietal network (FPN; Braunlich, Gomez-Lavin, & Seger, 2015) and salience networks (SN; Liang, Zou, He, & Yang, 2016), with specific functional network sub-regions flexibly adapting their activity and connectivity to increased working memory demands (Schlosser, Wagner, & Sauer, 2006; Xu, Calhoun, Pearlson, & Potenza, 2014). Recent work has suggested that default mode network (DMN) functional connectivity in the posterior cingulate cortex (PCC) may also modulate with working memory task performance (Esposito et al., 2009; Hampson, Driesen, Skudlarski, Gore, & Constable, 2006; Spreng et al., 2014). Further, the functional connectivity of the bilateral angular gyri, additional DMN-associated regions, has been found to increase as working memory task demands intensify (Vatansever, Manktelow, Sahakian, Menon, & Stamatakis, 2016; Woodward et al., 2006).

Given the significant FPN and DMN inter-network coordination necessary for proper working memory task performance, particularly at higher working memory loads, we reasoned that the working memory deficits and related complaints from patients after cardiac surgery may reflect postoperative changes in these large-scale functional networks due to embolic damage and/or neuroinflammation. We previously reported a positive relationship between resting-state functional connectivity changes in the left ventral posterior cingulate cortex (vPCC; Brodmann 23) and right superior frontal gyrus (SFG) and global postoperative cognitive changes after cardiac surgery (Browndyke et al., 2017). It is unclear, however, if these same regional functional connectivity network changes are manifest in cardiac surgery patients during postoperative task performance.

To examine this possibility, we performed detailed cognitive testing and functional neuroimaging during a working memory (N-back) task in patients before and after cardiac surgery, and at the same time intervals in non-surgical controls. We used two voxel-wise whole brain graph theory-based functional connectivity metrics to assess for perioperative changes in working memory load-associated functional connectivity between groups over time. Intrinsic Connectivity Contrast (ICC), a voxel-wise connectivity metric assessing degree centrality [i.e., "edges" (internode connections) for a particular locus or node], characterizes the magnitude of the global connectivity pattern between each voxel and the rest of the brain (Constable et al., 2013; Lee et al., 2014; Martuzzi et al., 2011; Scheinost et al., 2012). ICC has been used to identify changes in degree centrality during resting-state and task-based functional connectivity paradigms associated with working

memory load (Vatansever et al., 2016), anesthetic states (Martuzzi et al., 2011), ischemic stroke (Yassi et al., 2015), seizure disorder (Lee et al., 2014), pediatric conditions (Constable et al., 2013), and more recently by our research group in association with resting-state functional imaging data and cognitive dysfunction after cardiac surgery (Browndyke et al., 2017). Integrated Local Correlation (ILC), another voxel-wise connectivity metric, is useful in determining the strength or change in the regional homogeneity or "local coherence" of functional networks (Deshpande, LaConte, Peltier, & Hu, 2009). ILC and similar approaches [e.g., regional homogeneity (Zang, Jiang, Lu, He, & Tian, 2004), local functional connectivity density (Tomasí and Volkow, 2010)] have been employed to assess local network connectivity alterations during anesthetic states (Deshpande, Kerssens, Sebel, & Hu, 2010), in psychiatric conditions (Guo et al., 2015; Liu et al., 2006), and in association with age-related neuropathology (Zhang et al., 2012).

We hypothesized that cardiac surgery patients would demonstrate postoperative alterations in degree centrality and local coherence in brain networks associated with working memory load. Alteration of degree centrality and local coherence in areas associated with the DMN and frontoparietal networks (FPN) would suggest possible working memory load-related dysfunction in large scale functional brain networks previously shown to modulate their activity in response to increased cognitive demands (Anticevic et al., 2012; Stanley et al., 2014; Vatansever et al., 2016) or that are critically involved in the manipulation or decision making functions of working memory task performances (Collette and Van der Linden, 2002; D'Esposito, 2007; Ekman, Fiebach, Melzer, Tittgemeyer, & Derrfuss, 2016). We also evaluated the hypothesis that surgery-related cerebrovascular damage due to particulate or gaseous embolization, assessed through perioperative changes in T2 FLAIR white matter hyperintensity volumes, may account for postoperative cognitive deficits and/or be related to task-based FC changes associated with increased working memory load. Furthermore, since working memory plays a key role in numerous neuropsychological processes (Kearney-Ramos et al., 2014), we also hypothesized that postoperative alterations in working memory load-associated FC would be associated with cognitive change after cardiac surgery.

## 2 | MATERIALS AND METHODS

This study was approved by the Duke University Medical Center (DUMC) Institutional Review Board (IRB) and the Duke Brain Imaging and Analysis Center (BIAC) scientific review committee. The research was conducted in accordance with the Code of Ethics of the World Medical Association (Declaration of Helsinki).

### 2.1 | Participants

Participants were recruited from DUMC cardiology and cardiac surgery clinics. After obtaining informed consent, patients over the age of 60 years scheduled to undergo coronary artery bypass grafting (CABG) and/or valve replacement (VR) surgery with cardiopulmonary bypass

TABLE 1 Demographic, general health factors, and surgical characteristics

	Variable	Group		p value <sup>c</sup>
		Surgical (n = 25)	Controls (n = 26)	
Demographics	Mean age, yrs. (SD) [range]	66.7 (6.8) [57–84.3]	67.2 (7.3) [55.1–83.9]	.89
	Sex (M/F)	13/12	23/3	.01*
	Education, yrs. (SD) [range]	15.8 (3.2) [12–20]	15.9 (2.5) [12–20]	.60
	Race (Afr.Amer/Cauc/Asian/Other)	1/21/3/0	1/25/0/0	.35
Health factors	Diabetes (Type I or II)	(7/25) 32%	(7/26) 26.9%	.99
	History of hypertension	(18/25) 72%	(21/26) 80.8%	.74
	Previous myocardial infarction	(4/25) 16%	(5/26) 19.2%	.73
	LVEF %, median (Q1, Q3)	55.0 (55.0, 55.0)	55.0 (55.0, 59.0)	1.00
	Baseline brain parenchymal fraction (SD) <sup>a</sup> [range]	0.70 (0.82) [0.65–0.77]	0.80 (1.10) [0.65–0.78]	.72
	Baseline white matter hyperintensity burden (SD) <sup>b</sup> [range]	0.91 (1.29) [0.06–3.34]	0.99 (1.48) [0.05–4.55]	.83
	NYHA Class 0/1/2/3	9/2/11/3	5/2/3/0	—
Surgical characteristics	#Coronary Grafts 0/1/2/3/4	17/1/4/1/2	—	—
	Surgical procedure	Valve (16), CABG(6), CABG + Valve (3)	—	—
	Mean pump CPB time, min. (SD) [range]	159.3 (63.7) [71–329]	—	—
	Mean cross clamp time, min (SD) [range]	84.0 (47.3) [0–227]	—	—

Note. Abbreviations: LVEF = left ventricular ejection fraction; CPB = cardiopulmonary bypass.

<sup>a</sup>Calculated as whole brain volume (mL)/total intracranial volume (mL).

<sup>b</sup>Calculated as [total white matter hyperintensity volume (mL)/whole brain volume (mL)] × 100.

<sup>c</sup>Independent, two-sample t test or Fisher exact test comparisons (two-tailed) as appropriate. LVEF analyzed using Wilcoxon Rank Sum test due to missing data in the controls (n = 9) and non-normality.

\*p < .05.

were prospectively enrolled. Similarly, nonsurgical ambulatory controls with a documented history of coronary disease, as evidenced by a prior history of myocardial infarction or cardiac catheterization, were consented to participate (Table 1). Controls could not be under consideration for percutaneous or surgical cardiac revascularization 6 weeks prior to or within the baseline study visit. A history of cardiac or non-cardiac surgery >6 weeks prior to study enrollment was allowed for both study groups. Control participants were not subselected from any larger sample for matching purposes. Patients and controls with a history of symptomatic cerebrovascular disease with substantial residual deficit, alcoholism, psychiatric illness, renal failure (creatinine > 2.0 mg/dl), a less than 7th grade education, inability to read (and thus unable complete neuropsychological testing), or with bodily implants unsafe for 3 T MRI were excluded. Additional exclusion criteria included a baseline Mini Mental Status Exam (MMSE; (Cockrell and Folstein, 1988) total score ≤26, and a Center for Epidemiological Studies – Depression Scale (CES-D (Lewinsohn, Seeley, Roberts, & Allen, 1997) score ≥27 (to rule out the presence of gross cognitive or mood dysfunction, respectively).

A subset of the nonsurgical ambulatory cardiac control and cardiac surgery participants with resting-state functional connectivity imaging data were analyzed separately and reported in Browndyke et al (2017).

## 2.2 | Perioperative management

General anesthesia was induced and maintained with midazolam, fentanyl, and isoflurane or sevoflurane. All surgical participants underwent non-pulsatile hypothermic (30°C–32°C) cardiopulmonary bypass with a membrane oxygenator and an arterial line filter. The bypass pump was primed with crystalloid, and serial hematocrit levels were maintained at ≥0.21. Before initiation of cardiopulmonary bypass, surgical patients received heparin anticoagulation (300–400 U/kg) to achieve a target activated coagulation time of >480 s. Perfusion was maintained at pump flow rates of 2–2.4 L min<sup>-1</sup> m<sup>-2</sup> throughout cardiopulmonary bypass to maintain mean arterial pressure at 50–80 mmHg. Arterial blood gases were measured every 15–30 min and used to maintain arterial carbon dioxide partial pressures of 35–40 mmHg (unadjusted for temperature (α-stat)), and oxygen partial pressures of 150–250 mmHg.

## 2.3 | Postoperative observation and management

Surgical participants were screened daily for agitation/sedation and postoperative delirium during the acute in-hospital recovery period on postoperative days 1–3. Possible alteration of patients' arousal level

was assessed using the Richmond Agitation-Sedation Scale (RASS; Sessler et al., 2002), while the presence of delirium was assessed using the Confusion Assessment Method for Intensive Care Units (CAM-ICU; Ely et al., 2001). The RASS and CAM-ICU were administered in standardized format by trained study technicians and supervised by a licensed clinical neuropsychologist (JNB).

Given known sensitivity of older individuals to anticholinergic medication side-effects (Fox et al., 2011) and the increased risk these medications pose for postoperative delirium (Campbell, Perkins, Hui, Khan, & Boustani, 2011; Han et al., 2001), anticholinergic medications were accounted for in each patient at each time point using in the Anti-cholinergic Cognitive Burden (ACB) scale developed by Boustani, Campbell, Munger, Maidment, and Fox (2008).

## 2.4 | Neurocognitive outcome measures

Participants were administered well-established and standardized neuropsychological assessment measures (Table 2) designed to assess auditory-verbal learning, immediate and delayed memory recall (Schmidt, 1996), visual immediate and delayed memory recall (Wechsler, 1987), auditory-verbal simple and complex attention (Wechsler, 1997), visuomotor performance and processing speed (Wechsler, 1997), manual dexterity (Trites, 2002), and complex executive functioning skills (Reitan, 1958). In addition, we employed a standardized non-phonemic word pronunciation task to estimate premorbid global intellectual functioning between groups (Wilkinson & Robertson, 2006; Casaletto et al., 2014). All assessment measures were administered in standardized format by trained study technicians and supervised by a licensed clinical neuropsychologist (JNB). Cognitive assessment at each study time point (e.g., presurgical baseline and 6 weeks follow-up) occurred just prior to the neuroimaging procedures detailed below.

## 2.5 | Neuroimaging procedures

All participants underwent standard MRI safety screening at each time point. Cardiac replacement valves and other implanted devices and materials were screened for 3 T MRI and total specific absorption ratio (SAR) safety limits.

## 2.6 | N-back working memory task

Participants performed a block-designed verbal N-back working memory task prior to and during MR scanning (Figure 1). Three successive fMRI runs were collected at each study visit (i.e., before surgery, and then 6 weeks after surgery). Participants practiced the verbal N-back working memory task prior to entering the scanner until they could complete the 2-back condition with  $\geq 80\%$  accuracy. This procedure was performed to avoid potential interpretative circularity issues that could be associated with simultaneous functional neuroimaging and task accuracy differences between groups. By reasonably minimizing any in-scanner N-back performances differences between groups, differences in task-based FC degree centrality and local coherence metrics between groups could be interpreted to reflect potential fundamental differences in how postoperative surgical patient and

nonsurgical control brains adapt to increasing working memory load at similar levels of task accuracy.

The N-back task was programmed and presented in E-prime (Ver. 2.0, Psychology Software Tools, Inc., Sharpsburg, PA) on a laptop computer during pre-scanning task practice, and on a desktop computer during MR scanning with task onset synchronized to fMRI sequence onset. The practice N-back and in-scanner N-back tasks differed in stimuli and condition block orders. The in-scanner working memory N-back task was presented on a projected screen and viewed by participants through a prism reflector attached to the head coil. Task stimuli consisted of black upper and lower case consonant letters centered on a white background. Each letter stimulus was presented for 500 ms. There was a four second instruction prompt at the beginning of each block, and a black cross-hair centered on a white background was presented during within-block interstimulus intervals (ISI; 2500 ms). Block capital and lower face consonants were used to control for possible visual priming effects that could influence working memory performance (Phillips-Bute et al., 2006; Silvis, Belopolsky, Murriss, & Donk, 2015). Randomly alternating 30-s blocks of 0-back, 1-back, and 2-back working memory conditions were presented during the prescan practice and over the three fMRI task runs for a total of nine blocks per N-back condition. Participant task responses during scanning were recorded via a MR-safe fiber optic 2-button box. Participants were instructed to press a yes or no button for each stimulus depending on whether or not it met the N-back task block instructions. Each task block contained 33% targets (i.e., correct yes responses) and 66% foils (i.e., correct no responses). Task accuracy, reflecting both correct yes and no stimuli responses, was recorded for both prescan practice and in-scanner task performance. Additionally, the number of prescan practice trials-to-criterion (e.g.,  $\geq 80\%$  accuracy for 2-back condition) was recorded.

The central objective of this study was to examine for changes in degree centrality and local coherence in response to increases in working memory load, accordingly we omitted the 0-back condition as a comparator because it does not impose demands upon working memory. Working memory load for all analyses reflects a direct contrast between 2-back and 1-back conditions.

## 2.7 | Neuroimaging data acquisition

Standard anatomical images and functional data were acquired on a 3 T General Electric MR750 MRI scanner with an 8-channel head coil. Anatomical data consisted of high-resolution T1-weighted fast spoiled gradient-echo (FSPGR; oblique axial acquisition,  $256 \times 256$  matrix, 256 mm FOV,  $11^\circ$  flip angle, 136 one-millimeter-thick slices, TE 3.0 ms, TR 6.93 ms) and T2 FLAIR (oblique axial acquisition,  $128 \times 128$  matrix, 256 mm FOV,  $90^\circ$  flip angle, 68 two-millimeter-thick slices, TE 145.6 ms, TR 11000 ms, TI 2250 ms) scans. Task-based N-back fMRI data were acquired over three separate runs using an SENSE spiral-in sequence (oblique axial, slice interleaved acquisition,  $64 \times 64$  matrix, 256 mm FOV,  $60^\circ$  flip angle, 24 four-millimeter-thick slices, TE 30 ms, TR 1500 ms, SENSE factor 2). Each fMRI run consisted of 220 time points (duration 5.5 min). Six initial time points (18 s) were discarded



TABLE 2 Cognition at baseline and postoperative change from baseline to 6 weeks

Cognitive variables <sup>a</sup>	Baseline performance		<i>p</i> <sup>c</sup>	6-week change <sup>b</sup>		<i>p</i> <sup>c</sup>
	Surgical ( <i>n</i> = 25)	Controls ( <i>n</i> = 26)		Surgical ( <i>n</i> = 25)	Controls ( <i>n</i> = 26)	
WRAT-4 Reading (SD) [range]	50.9 (5.9) [43–58]	50.4 (5.3) [44–57]	.73	–	–	–
RAVLT – initial learning (SD) [range]	5.84 (1.84) [2–9]	6.04 (1.97) [2–10]	.71	–0.09 (0.85) [–2.15, 1.52]	0.01 (1.04) [–2.15, 2.91]	.71
RAVLT – total learning (SD) [range]	51.16 (8.42) [41–66]	48.12 (11.25) [33–69]	.28	–0.49 (1.00) [–2.89, 1.78]	0.11 (0.96) [–1.79, 2.24]	.03*
RAVLT – delayed recall (SD) [range]	11.12 (2.68) [6–15]	9.11 (4.30) [3–15]	.05	–0.43 (1.06) [–3.45, 0.99]	0.07 (1.06) [–1.60, 3.22]	.10
WDSF – total correct (SD) [range]	8.28 (1.74) [4–11]	7.58 (2.10) [5–13]	.20	–0.09 (0.78) [–2.05, 1.24]	–0.08 (0.94) [–2.05, 2.18]	.97
WDSB – total correct (SD) [range]	7.32 (2.17) [4–12]	6.46 (2.19) [4–12]	.17	–0.19 (0.96) [–2.02, 2.12]	0.02 (1.01) [–2.02, 2.12]	.45
TMT – trails B (inverse log) (SD) [range]	–4.44 (0.39) [–5.49, –3.85]	–4.45 (0.38) [–5.15, –3.61]	.88	–0.93 (1.14) [–3.89, 0.80]	0.02 (1.03) [–2.12, 1.95]	.003**
DSST – total correct (SD) [range]	46.36 (11.05) [28–64]	52.38 (10.73) [30–65]	.05	–0.46 (1.06) [–2.90, 1.49]	–0.07 (1.00) [–0.64, 2.40]	.18
GPT – mean bilateral speed (inverse) (SD) [range]	–94.24 (29.73) [–204.5, –61.0]	–89.46 (29.14) [–214.5, –55.0]	.74	–0.41 (1.02) [–3.89, 1.11]	–0.18 (0.85) [–1.83, 1.45]	.38
Global cognitive change <sup>d</sup> (SD) [range]	–	–	–	–0.29 (0.38) [–1.51, 0.30]	0.01 (0.45) [–0.66, 0.76]	.01*

<sup>a</sup>Duke Neurologic Outcomes Research Group (NORG) Neurocognitive Battery [Wide Range Achievement Test (4<sup>th</sup> Revision) Reading Subtest (WRAT-4; Casaletto et al., 2014; Wilkinson, 2006); Rey Auditory Verbal Learning Test (RAVLT; Schmidt, 1996); Wechsler Adult Intelligence Scale – 3<sup>rd</sup> Revision Digit Span Forward (WDSF) and Digit Span Backward (WDSB) Subtests (Wechsler, 1997); Trail Making Test (TMT; Reitan, 1958); Wechsler Adult Intelligence Scale – 3<sup>rd</sup> Revision Digit Symbol Substitution Test (DSST; Wechsler, 1997); Lafayette Grooved Pegboard Test (GPT; Trites, 2002)].

<sup>b</sup>Expressed as reliable change index (RCI; Duff, 2012; Sawrie et al., 1996) scores relative to nonsurgical control group cognitive test–retest at 6 weeks and 1 year.

<sup>c</sup>Independent, two-sample *t* test comparisons (two-tailed).

<sup>d</sup>Calculated as the mean of RCI values from all cognitive variables.

\**p* < .05; \*\**p* < .01.

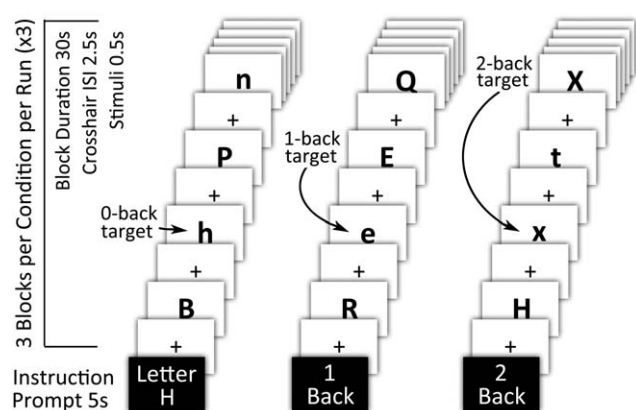


**FIGURE 1** Visual-orthographic N-back working memory task schematic. Note. All participants completed three N-back working memory task runs during neuroimaging data acquisition. Each fMRI run consisted of alternating blocks of 0-back (letter identification task), 1-back (low demand working memory task), and 2-back (high demand working memory task); 30-s block duration for each condition and 10-letter stimuli per block. Responses were required for all stimuli, targets, and foils. Each condition block contained 33% targets and 66% foils. N-back task accuracy was recorded for all conditions

from the beginning of each fMRI run to correct for initial MR signal fluctuation.

## 2.8 | Neuroimaging data preprocessing

Neuroimaging data were spatially preprocessed and analyzed using Statistical Parametric Mapping (SPM12, Wellcome Institute, London) software and SPM-based functional connectivity CONN Toolbox (Ver. 16b; McGovern Institute for Brain Research, Massachusetts Institute of Technology, Boston, MA) in MATLAB (Ver. 2014a; MathWorks, Natick, MA). T1 and T2 FLAIR anatomical data was first rough affine co-registered to Montreal Neurologic Institute (MNI) common atlas space. T1 anatomical data were then segmented to produce grey and white matter and CSF maps and a skull-stripped anatomical volume mask for each participant. These segmentation maps were retained for calculation of total intracranial volume (TIV) and for signal correction and masking procedures detailed below. Functional data were first screened for signal artifact (SPM ART toolbox), then slice-time corrected to the middle-slice of each acquisition. Functional data were then realigned to the first volume of each acquisition/session. Resulting movement parameter data were retained as covariates for subsequent data processing. Participant slice-time corrected and realigned functional data were then co-registered to respective T1 anatomical data and masked with the skull-stripped volume from anatomical data segmentation. SPM anatomical segmentation parameters were then applied to both the T1 anatomical segmented and co-registered T2 FLAIR and functional data for nonlinear alignment with MNI atlas space (2 mm isotropic voxels). Functional data were spatially smoothed with a Gaussian 8 mm full width at half maximum filter. White matter lesion volume was measured from co-registered and normalized T1 and longitudinally bias-corrected T2 FLAIR data for each time point using the

MATLAB Lesion Segmentation Toolbox (LST) (Schmidt et al., 2012). Lesion segmentation thresholds were first determined by selecting a random sample of ten bias-corrected T2 FLAIR images from surgical patients and controls, which were then passed through the threshold free LST lesion prediction algorithm (LPA). The resulting LPA-generated lesion maps were then manually edited to correct for any lesion territories not identified or misclassified to establish lesion ground truth images. Using these edited ground truth images as guides, we then determined the optimal kappa ( $k$ ) for the LST Toolbox seed region legion growth algorithm (LGA) via iterative examination of dice coefficients between the edited ground truth lesion images and LGA-generated lesion belief maps at various  $k$  settings and through additional visual inspection by an individual blind to group assignment (PJS). An optimal LGA  $k$  setting of 0.3 was associated with 80.7% sensitivity and 98% specificity. The remainder of the longitudinally bias-corrected T2 FLAIR data was then LGA processed at this optimal kappa setting to derive whole brain white matter hyperintensity volumes for each subject at each time point.

Each participants' fMRI data were denoised through linear regression of confounding effects including subject motion, BOLD signal artifacts (i.e., scan-to-scan global signal 3.00  $z$  value threshold; composite motion threshold, 0.5 mm), BOLD signal in CSF and white matter (via aCompCor method; Behzadi, Restom, Liao, & Liu, 2007), and main effects of all N-back task-condition blocks via a hemodynamic response functions (HRF)-modeled with first-order temporal derivative. After signal confound removal, the resulting functional data were high-pass filtered using standard settings for task-based functional data analyses (i.e., 1/128 Hz). BOLD signal session-specific temporal linear detrending was performed after confound removal regression. Principal components decomposition analysis was performed after removal of first-level confound covariates, and 64 singular value decomposition (SVD) components were used for subject-level dimensionality reduction for ICC and ILC analyses (see *Intrinsic Connectivity Contrast & Integrated Local Correlation* sections below; Whitfield-Gabrieli and Nieto-Castanon, 2012).

## 2.9 | Analyses

### 2.9.1 | Demographic variables, cognitive outcomes, and perioperative management

Independent, two-sample  $t$  tests or Fisher exact tests (where appropriate) were used to compare demographic variables and to assess differences in cognitive outcomes between groups. A  $p$  value  $< .05$  (two-tailed) was chosen for statistical significance. Cognitive comparisons were performed on raw neurocognitive test scores at the baseline visit, and on calculated reliable change indices (RCI) at subsequent follow up visits. RCIs were calculated for both groups using change in cognitive performance in controls as a comparator. RCI values were calculated by the equation  $(T_2 - T_1) - (M_2 - M_1)/SED$ , where  $T_1$  equals the baseline score,  $T_2$  is the score at 6 week follow-up,  $M_1$  is the control group score mean at baseline,  $M_2$  is the control group score mean at follow-up, and SED is the control group standard error of difference. SED was calculated as  $\sqrt{[(S_1(\sqrt{1 - r_{12}}))^2 + (S_2(\sqrt{1 - r_{12}}))^2]}$ , where  $S_1$  is

the control baseline standard deviation,  $S_2$  is the control follow-up standard deviation, and  $r_{12}$  is the correlation coefficient between baseline and follow-up scores in the control group. The resulting RCI values reflect a  $z$  distribution of the magnitude of cognitive change from baseline, and control for normal test-retest variability and practice effects (Duff, 2012; Sawrie, Chelune, Naugle, & Luders, 1996). Mean global RCI, calculated as the average of all eight cognitive variable RCIs (Table 2), was used as an aggregate measure of global postoperative cognitive change and is similar to a continuous cognitive change index that we have previously reported in cardiac and non-cardiac surgery cognitive outcome studies (Mathew et al., 2013; McDonagh et al., 2010; Newman et al., 2001b).

Evaluation of group differences in Anticholinergic Cognitive Burden Scale (ACB) (Boustani et al., 2008) medication frequencies at baseline and follow-up were conducted via generalized linear mixed model with binomial distribution (two-tailed  $p$  value  $< .05$ ).

### 2.9.2 | Corrected whole brain and white matter lesion volumes

T1 anatomical tissue segmentation at presurgery baseline was used to calculate total parenchymal brain volume for each participant. Brain parenchymal fraction was calculated as whole brain volume (mL)/total intracranial volume (mL) and were compared between groups at baseline using an independent samples  $t$  test. T2 FLAIR variables of interest were total lesion volume (mL) and corrected white matter lesion burden [i.e., corrected white matter lesion burden = total lesion volume/total intracranial volume]. Independent, two-sample tests were conducted between groups for baseline lesion burden and pre-/postoperative changes (or 6-week natural changes in controls) in total lesion volume and corrected white matter lesion burden. Regression analyses, controlling for age, education, and gender, were also conducted in the surgical group to identify any potential relation between baseline variables and postoperative cognitive change, and any relations between lesion variable change and cognitive change. Within these analyses, predictors were scaled using the interquartile range. Statistical significance was set as  $p < .05$  (two-tailed) for all brain volume and lesion-related analyses.

### 2.9.3 | Intrinsic connectivity contrast and integrated local correlation

The ICC metric is expressed as  $\frac{1}{|\Omega|} \sum_{y \in \Omega} |r(x, y)|^2$  where  $r(x, y)$  represents the voxel-to-voxel connectivity matrix for any two spatially arbitrary voxels  $x$  and  $y$ , and  $\Omega$  is the set of all brain voxels. ICC data reflect the magnitude of degree centrality independent of sign and are expressed as absolute  $R^2$  values, thus eliminating the need for arbitrary weighting thresholds. Prior to GLM analyses, raw ICC values were Gaussian distribution normalized for each voxel to  $z$  scores reflecting mean level of connectivity across all other voxels, separately for each participant/condition. Post-hoc seed-to-voxel examination of any significant ICC findings were conducted to determine contributing areas and the sign (positive or negative) of their correlative input (Vatansever et al., 2016; Whitfield-Gabrieli & Nieto-Castanon, 2012).

The integrated local correlation (ILC) metric characterizes the average local connectivity between each voxel and its neighbors. (Deshpande et al., 2009). ILC is expressed as  $\sum_{y \in \Omega} h_{\sigma}(x - y) \cdot r(x, y)$  where  $r$

$(x, y)$  is the voxel-to-voxel connectivity matrix constrained to local correlations within a Gaussian convolution kernel ( $h$ ) with a width ( $\sigma$ ), and  $\Omega$  is the set of all brain voxels. An 8 mm spatial convolution kernel was used for ILC bounds.

A two-stage partitioned variance approach mixed within-/between-subjects ANCOVA model (Henson, 2015; Henson and Penny, 2005) was used to examine for a three-way interaction in ICC and ILC values between groups (i.e., between-subject factor; surgical patients > nonsurgical controls) and two within-subject factors (e.g., time = 6-week > baseline; and working memory load = 2-back > 1-back). In this two-stage analysis approach, within-subject time  $\times$  working memory load change contrast maps were first computed for each subject, after which they were entered into a second-level, random effects two-sample  $t$  test analysis with covariates in SPM12. We adjusted for possible confounding effects of sex (given group differences in this demographic variable; see Table 1), white matter hyperintensity volume change from baseline to 6 weeks, and in-scanner N-back performance change from baseline. For all analyses, change in task-based degree centrality (ICC) and local coherence (ILC) associated with working memory load was expressed as the 6 week follow-up minus the baseline, resulting in positive normalized  $z$  values for postoperative increases in degree centrality and local coherence, and vice versa. Post-hoc analyses with the same demographic, lesion and task performance covariates were conducted to examine for simple main effects contributing to any omnibus three-way interaction analysis results. In addition, mean contrast values were extracted for each  $n$ -back condition at each time point for visualization of individual task conditions contributing to any regional three-way interaction working memory load change between groups.

All ICC and ILC analyses were conducted with a primary cluster-defining, peak voxel threshold  $p < .001$  and family-wise cluster-corrected spatial extent ( $k_E$ ) threshold  $p\text{-FWE} < .05$ .

### 2.9.4 | Post-hoc seed-to-voxel examination of degree centrality metric findings

Significant regions identified by the ICC analyses described above were then used as source regions-of-interest (ROIs) for within-group seed-to-voxel task-based FC analyses. ICC analyses provide data about voxel-wise differences in the magnitude of degree centrality change for any particular significant region, but do not specify which connecting regions or networks account for any significant ICC findings. Thus, post-hoc seed-to-voxel analyses were conducted to examine for the contributing regions accounting for significant regions identified by ICC. The time series of interest in these post-hoc task-based FC analyses was the average BOLD signal within the seed ICC ROIs. Seed ROIs only included BOLD signal within participants' gray matter segmentation masks. Each seed ROI was interrogated for bivariate correlation (Fisher  $Z$  normalized  $r$  values) with BOLD signal throughout the rest of the brain via first-level HRF function with temporal derivative weighted generalized linear model analyses (Whitfield-Gabrieli & Nieto-Castanon, 2012). Resulting participant seed-to-voxel first-level correlation maps were then entered into random-effects, within-group paired  $t$ -test analyses of baseline to 6-week task-based FC changes associated with increased working memory load (2-back > 1-back). These analyses



**TABLE 3** Regions of significant working memory load-associated degree centrality and local coherence change from baseline to 6-week follow-up in cardiac surgery patients and nonsurgical controls

Connectivity metric <sup>a</sup>	Locus (Brodmann areas) <sup>b</sup>	$k_E$	SPM <sub>T</sub>	Local maxima <sup>c</sup>		
				x	y	z
Degree centrality (intrinsic connectivity contrast; ICC)	Left dorsal posterior cingulate cortex (BA 31)	156	4.59	−10	−70	30
			4.52	−2	−70	34
			4.36	0	−60	36
Local coherence (integrated local correlation; ILC)	Left and right dorsal posterior cingulate cortex (BA 31)	89	4.23	−2	−66	38
			3.72	6	−66	28

<sup>a</sup>Statistical parametric mapping (SPM) mixed within-/between-subjects ANCOVA (Henson, 2015; Henson and Penny, 2005) of tbfMRI voxel-wise intrinsic connectivity change (or integrated local correlation change) values between groups and two within-subject factors (i.e., time and working memory load; i.e., 2 > 1-back), adjusting for sex, perioperative global white matter hyperintensity volume change, and N-back performance accuracy change [surgical patients ( $n = 25$ ), controls ( $n = 26$ ); cluster-defining peak voxel threshold  $t \geq 3.29$  ( $p < .001$ ) and family-wise error-corrected cluster spatial extent threshold ( $k_E$ )  $p\text{-FWE} < .05$ ].

<sup>b</sup>Anatomical and Brodmann area labels based upon 7 mm<sup>3</sup> search range of the Talairach Daemon Database using MNI-to-Talairach nonlinear transform coordinates (Lancaster et al., 2000).

<sup>c</sup>Montreal Neurological Space (MNI) ICBM152 nonlinear 6th generation brain atlas coordinates.

were performed on each statistically significant ICC seed ROI, and were adjusted for sex, N-back task accuracy change, and white matter lesion volume change.

These post-hoc seed-to-voxel analyses were conducted for explanatory signal contributions; thus, all post-hoc seed-to-voxel analyses were conducted with the same statistical thresholds as our original ICC and ILC analyses. Any results from these post-hoc seed-to-voxel analyses were not interpreted as having statistical significance beyond the original ICC analysis thresholds.

Intrinsic functional networks associated with any significant ICC or ILC analysis regions, and any contributors to the omnibus ICC analysis, were determined using Neurosynth (<http://neurosynth.org>); an open-source neuroimaging meta-analytic tool comprised of the activation coordinates and associated study subject terms from over 11406 peer-reviewed functional imaging studies. (Yarkoni, Poldrack, Nichols, Van Essen, & Wager, 2011) Functional connectivity and meta-analytic coactivation correlation values associated with the search terms “working memory, executive control, frontoparietal network, and default mode network” were generated by Neurosynth and used to determine the likelihood of working memory and default mode-associated large scale functional networks for the local maxima of any regions found in ICC or ILC analyses (Table 3) and any contributing regions to significant ICC analysis results (Table 4).

Post-hoc seed-to-voxel analyses were not conducted for ILC analyses as this functional connectivity metric already reflects constrained, localized coherence changes within any significant ILC foci finding.

### 2.9.5 | Linear regression of task-based FC analysis results, global cognitive outcome, and N-back accuracy

Linear regression analyses were conducted for significant 6-week ICC and ILC findings to examine for relationships between any perioperative working memory load-associated degree centrality or local coherence changes and global cognitive outcomes (as expressed by mean

global RCI values; see Table 2). We also examined the relationship between the same 6 week task-based degree centrality and local coherence changes and in-scanner N-back task accuracy change from baseline to 6 weeks for 1-back and 2-back conditions.

All regression analyses were conducted with a statistical significance threshold ( $p < .05$ ; two-tailed) determined relative to a null relationship slope.

## 3 | RESULTS

Two surgical and one control participant were excluded from task-based FC analyses due to a high number of BOLD signal outliers and/or excessive movement at presurgery baseline or 6 week follow-up. Thus, 25 surgical and 26 control participants were included in the primary analyses of baseline to 6 week task-based FC change.

### 3.1 | Demographic, health, and surgical variables

Baseline demographic characteristics of the cardiac surgery and non-surgical control participants were similar with the exception of gender [surgical 12 female, control 3 female;  $p = .01$ ; see Table 1], which was thus retained as a covariate in task-based FC analyses. There were no significant differences between groups in baseline brain parenchymal fraction [i.e., whole brain volume (mL)/total intracranial volume (mL)] or in brain volume-adjusted total white matter hyperintensity burden [i.e., (total white matter hyperintensity volume (mL)/whole brain volume (mL))  $\times 100$ ; see Table 1]. Additional patient characteristics and intraoperative variables in the surgical patients are listed in Table 1.

### 3.2 | Baseline and postoperative cognitive outcomes

There were no statistically significant differences between groups in baseline cognitive performance. The RCI of two cognitive variables were significantly different between groups at 6 weeks. The surgical

**TABLE 4** Regions contributing to significant degree centrality working memory load group  $\times$  time interaction difference foci (Figure 3)

ICC seed/ROI <sup>a</sup>	Directionality of task-based FC change	Locus (Brodmann areas) <sup>b</sup>	$k_E$	SPM <sub>T</sub>	Local maxima <sup>c</sup>		
					x	y	z
Left dorsal posterior cingulate cortex (BA 31)	Increase	Right inferior frontal gyrus (BA 47)	85	5.53	22	16	-20
		Left dorsal posterior cingulate cortex (BA 31)	69	5.44	-2	-66	34
		Right caudate nucleus	75	4.79	10	14	0
		Left superior frontal gyrus (BA 6)	63	4.61	-56	4	36
		Left postcentral gyrus (BA 1)	50	4.48	-38	-30	50
		Left inferior temporal gyrus (BA 37)	41	4.22	-56	-68	-6
	Decrease	Right superior parietal lobule (BA 7)	47	4.66	20	-62	66

<sup>a</sup>Post-hoc, statistical parametric mapping (SPM) mixed within-/between-subjects ANCOVA (Henson, 2015; Henson and Penny, 2005) analysis of group (surgery, control)  $\times$  time (baseline, 6 weeks)  $\times$  condition (working memory load, 2 > 1-back) interaction, adjusting for gender, perioperative global white matter hyperintensity volume change, and N-back performance accuracy change, using ROI seeds from omnibus intrinsic connectivity change (ICC) analyses (Table 3) [surgical patients ( $n = 25$ ), controls ( $n = 26$ ); cluster-defining peak voxel threshold  $t \geq 3.29$  ( $p < .001$ ), family-wise error-corrected cluster spatial extent ( $k_E$ ) threshold  $p\text{-FWE} < .05$ ].

<sup>b</sup>Anatomical and Brodmann area labels based upon 7 mm<sup>3</sup> search range of the Talairach Daemon Database using MNI-to-Talairach nonlinear transform coordinates (Lancaster et al., 2000).

<sup>c</sup>Montreal Neurological Space (MNI) ICBM152 nonlinear 6th generation brain atlas coordinates.

group showed worsened postoperative auditory-verbal list learning [RAVLT total learning; surgical RCI -0.49 (1.0), control RCI 0.11 (0.96);  $p = .03$ ] and decreased executive functioning [Trail Making Test (TMT) - Trails B; surgical RCI -0.93 (1.14), control RCI 0.02 (1.01);  $p = .003$ ]. In addition, the global cognitive performance at 6 weeks in the surgical participants, calculated as the mean total RCI for all cognitive variables, declined significantly relative to controls [surgical mean total RCI -0.29 (0.38), control mean total RCI 0.01 (0.45);  $p = .01$ ] (Table 2).

### 3.3 | Postoperative delirium, arousal, and medication variables

None of the surgical patients screened positive for delirium on the CAM-ICU (Ely et al., 2001) during the 3-day, acute in-hospital recovery observation period, although two patients selectively tested positive for the CAM inattention feature on postoperative day 1. No CAM-ICU screened delirium features screened positive on postoperative days 2 and 3. Three surgical patients had RASS (Sessler et al., 2002) scores <0, indicative of light sedation or decreased level of consciousness, on day 1, while two of these three patients also had additional RASS scores <0 on postoperative recovery day 2.

Binary scores were assigned for the presence or absence of anticholinergic medications listed in the Anticholinergic Cognitive Burden (ACB) scale (Boustani et al., 2008) at baseline and follow-up for each study group. 68% of surgical patients were prescribed ACB-listed medications at baseline and 52% at 6 week postoperative follow-up. Conversely, 38% of controls were prescribed ACB-listed medications at baseline and 57% at 6 week follow-up. Using these ACB medication frequencies, a generalized linear mixed model with binomial distribution was conducted to evaluate for group differences. There were no statistically significant effects in ACB-listed medications for group ( $p = .14$ ), time ( $p = .76$ ), or group-by-time interaction ( $p = .09$ ).

### 3.4 | N-back task performance

There were no significant differences between groups in the number of N-back practice trials required to reach prescan performance criterion (i.e.,  $\geq 80\%$  accuracy for all N-back task conditions) at presurgery baseline [surgical 2.12 (1.27), control 1.77 (1.27),  $p = .44$ ] or 6 week follow-up [surgical 1.28 (0.61), control 1.11 (0.32),  $p = .23$ ]. Similarly, there were no statistically significant differences between groups for in-scanner N-back task accuracy at baseline [0-back accuracy: surgical 95.68 (4.22), control 97.27 (2.35),  $p = .10$ ; 1-back accuracy: surgical 94.02 (6.26), control 93.88 (4.44),  $p = .92$ ; 2-back accuracy: surgical 86.67 (8.71), control 87.89 (8.23),  $p = .61$ ] or 6 week follow-up [0-back accuracy: surgical 97.85 (2.75), control 97.73 (2.53),  $p = .89$ ; 1-back accuracy: surgical 96.27 (4.04), control 95.52 (4.80),  $p = .55$ ; 2-back accuracy: surgical 89.58 (7.45), control 89.20 (8.11),  $p = .86$ ].

### 3.5 | Corrected whole brain and white matter lesion volumes and cognitive changes

There were no significant differences between groups in baseline brain parenchymal fraction [surgical 0.73 (0.03), control 0.72 (0.04);  $p = .29$ ] or in whole brain volume-corrected presurgery ischemic white matter disease burden [surgical 0.91% (1.29), control 0.99% (1.48);  $p = .83$ ; see Table 1]. No significant differences in total white matter hyperintensity volumes were found between groups at baseline [surgical 7.42 mL (9.09), control 7.91 mL (10.05),  $p = .86$ ] or 6 weeks [surgical 7.65 mL (9.23), control 8.05 (10.33),  $p = .88$ ]. Similarly, a ratio measurement of total white matter hyperintensity volume (mL) to whole brain volume (mL) was not statistically significant between groups at baseline [surgical 0.70 (0.82), control 0.80 (1.10),  $p = .72$ ] or follow-up [surgical 0.72 (0.83), control 0.81 (1.13),  $p = .75$ ].

Among the surgical group and controlling for age, education, and gender, neither baseline white matter lesion volume nor burden were associated with overall cognitive change ( $R^2 = 0.23$ ,  $p = .17$ ). Greater white matter volume at baseline was associated with lower total AVLT performance at 6 weeks ( $b = -0.22$ ,  $p = .047$ ). In ancillary analyses examining surgical factors as predictors of baseline to 6 week cognitive change, greater cardiopulmonary bypass pump time was associated with worse performance on the Grooved Pegboard test ( $b = -0.59$ ,  $p = .027$ ).

### 3.6 | Voxel-wise intrinsic functional connectivity

To identify potential brain regions associated with differential working memory-load (2-back > 1-back) degree centrality changes from baseline to 6 weeks between groups, we performed a mixed within-/between-subjects ANCOVA on the ICC data using a two-stage partitioned variance approach (Henson, 2015; Henson and Penny, 2005). The results of this interaction analysis identified a region in the left dorsal posterior cingulate cortex (dPCC) with three local maxima [cluster 156  $k_E$ ; 4.59T (MNI  $-10x$ ,  $-70y$ ,  $30z$ ), 4.52T (MNI  $-2x$ ,  $-70y$ ,  $34z$ ), 4.36 (MNI  $0x$ ,  $-60y$ ,  $36z$ )] that exceeded our cluster-forming ( $p < .001$ ) peak threshold and family-wise error-corrected cluster extent threshold ( $p\text{-FWE} < .05$ ) (Table 3 and Figure 2A). Post-hoc analyses of working memory load contrast differences between groups, as well as analyses of simple main effects differences between groups for 1-back and 2-back task conditions, were conducted for each time point. Additionally, potential group differences associated with 1-back and 2-back condition change over time were examined (e.g., 6-week 2-back > baseline 2-back). These explanatory post-hoc analyses controlled for the same demographic, lesion and  $n$ -back performance factors and had the same statistical thresholds as the primary interaction model. No statistically significant regions were found between groups for 1-back, 2-back or working memory load (2- > 1-back) at presurgical baseline or in the change in 1-back over time. A significant simple main effect for 2-back condition between groups was found in the dPCC region postoperatively at 6-weeks follow-up (cluster 128  $k_E$ ; 4.46T, MNI  $-12x$ ,  $-80y$ ,  $32z$ ) and in the change in 2-back over time between groups (cluster 78  $k_E$ ; 4.13T, MNI  $-8x$ ,  $-68y$ ,  $30z$ ), and for postoperative working memory load contrast (cluster 98  $k_E$ ; 3.71T, MNI  $0x$ ,  $-72y$ ,  $32z$ ). Mean ICC values for each  $n$ -back condition were plotted by group and time for visualization of effects contributing to the significant group  $\times$  time  $\times$  condition interaction (Figure 2C).

### 3.7 | Voxel-wise integrated local correlation

A single region spanning the left and right dorsal posterior cingulate cortex (dPCC; see Table 3) was found to exceed statistical thresholds in a mixed within-/between-subjects ANCOVA analysis using a two-stage partitioned variance approach similar to that conducted for ICC data. This significant interaction analysis ILC locus had two local maxima; one in each cerebral hemisphere [cluster 89  $k_E$ ; 4.23 T ( $-2x$ ,  $-66y$ ,  $38z$ ), 3.72 T ( $6x$ ,  $-66y$ ,  $28z$ )]. Post-hoc analyses of ILC simple main effects of  $n$ -back condition and working memory load contrast at

each time point, as well as  $n$ -back condition change differences between groups over time, revealed only a significant difference in ILC between groups in the 2-back condition over time (surgery > control; cluster 123  $k_E$ , 3.78 T, MNI  $-8x$ ,  $-62y$ ,  $26z$ ).

### 3.8 | Large-scale functional network association for significant ICC and ILC analysis foci

A Neurosynth database (Yarkoni et al., 2011) search of whole-brain reverse inference map functional connectivity and meta-analytic co-activation using the local maxima from the significant dPCC ICC and ILC foci (Table 3) revealed the dPCC is most strongly associated with the default mode network (dPCC locus  $r = 0.48$ , meta-analytic co-activation  $r = 0.45$ ) and weakly inversely associated with working memory and associated large scale networks (e.g., FPN). Similarly, the dPCC ILC local coherence change foci was strongly associated with the default mode network ( $r = 0.49$ , meta-analytic co-activation  $r = 0.45$ ) and inversely associated with working memory and associated network terms.

### 3.9 | Determination of contributing regions to significant ICC analysis foci

The significant dPCC ICC cluster demonstrating significant differences for increased working memory load between groups and time (Table 3 and Figures 2A and 3A) was used as a seed ROI in post-hoc, random-effects seed-to-voxel analyses utilizing the adjustment factors from the original ICC analysis. This post-hoc analysis was conducted to identify brain regions that contributed to the ICC findings, and the directionality of their relationship with the degree centrality changes described above.

The dorsal posterior cingulate cortex (dPCC) ICC cluster (Table 3 and Figure 2A) finding was accounted for by both increased and decreased task-based functional connectivity for working memory load between this seed ROI and seven contributing regions (Table 4 and Figure 3). A similar Neurosynth database search of large scale network functional connectivity and meta-analytic co-activation using the local maxima from these contributing regions and the aforementioned four search terms showed that these regions were variably associated with the working memory-related and default mode networks. Of the six identified regions that demonstrated increased working memory load-associated task-based FC to the dPCC ICC locus, two were most associated with the default mode (e.g., left dPCC,  $r = 0.48$ , meta-analytic coactivation,  $r = 0.45$ ; right caudate,  $r = 0.20$ , meta-analytic coactivation,  $r = 0.01$ ); two were associated with working memory and/or associated networks (e.g., left superior frontal gyrus,  $r = 0.13$ , meta-analytic coactivation,  $r = 0.38$ ; left inferior temporal gyrus,  $r = 0.18$ , meta-analytic coactivation,  $r = 0.15$ ); while the remaining two were neither positively associated with default mode nor working memory-related search terms (e.g., right inferior frontal gyrus, left precentral gyrus). The sole contributor to the dPCC ICC finding that decreased in functional connectivity in association with working memory load was a region

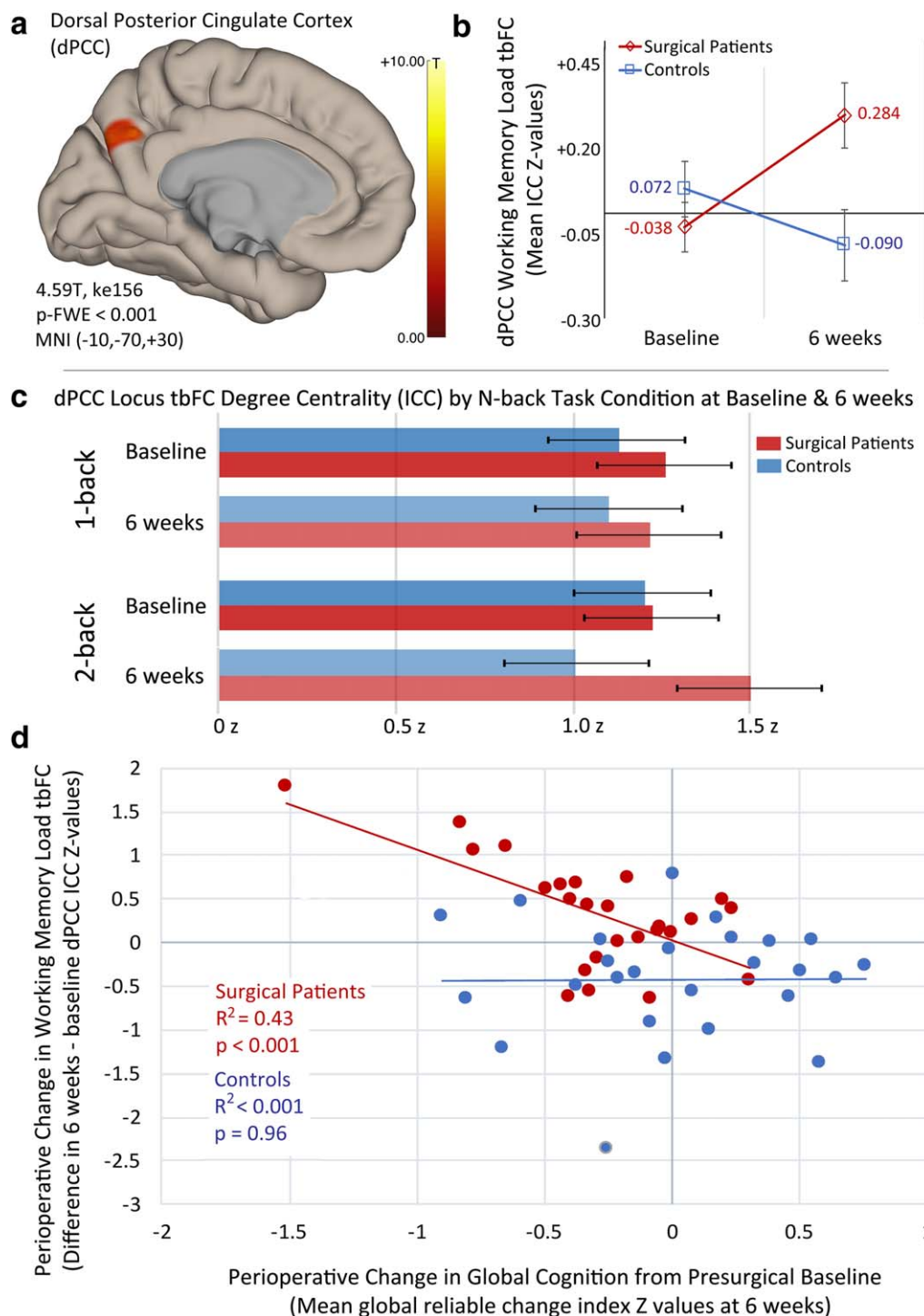


**FIGURE 2** Working memory load-associated degree centrality changes in the dorsal posterior cingulate of cardiac surgical patients and nonsurgical controls and its relationship with postoperative global cognitive change. *Note.* (a) Statistically significant task-based functional connectivity (tbFC) voxel-wise intrinsic connectivity contrast (ICC) change in the dorsal posterior cingulate cortex (dPCC) associated with working memory load (i.e., 2-back > 1-back) in surgical patients relative to controls, adjusting for sex, perioperative global white matter hyperintensity volume change, and N-back performance accuracy [surgical patients ( $n = 25$ ), controls ( $n = 26$ ); cluster-defining peak voxel threshold  $t \geq 3.29$  ( $p < .001$ ), family-wise error-corrected cluster spatial extent ( $k_E$ ) threshold  $p\text{-FWE} < .05$ ; see Table 3]. (b) Changes in tbFC ICC measured degree centrality during increased working memory load in the dPCC foci (a) at presurgical baseline and postoperatively at 6 weeks in surgery patients and nonsurgical controls (y-axis = difference in normalized ICC z-values for 2-back > 1-back; error bars reflect 90% confidence interval). (c) tbFC dPCC degree centrality, as measured by normalized ICC z values, for each n-back condition contributing to the working memory load contrast (2-back > 1-back) by group and time; error bars reflect 90% confidence interval. (d) Relationship between working memory load-associated degree centrality change in the dPCC foci (a) from baseline to 6 weeks and change in global cognition in surgical patients and nonsurgical controls [x-axis = change in working memory load associated ICC z-values in the dPCC at 6 weeks > baseline; y-axis = mean global reliable change index (z values) at 6 weeks relative to baseline; see Table 2] [Color figure can be viewed at [wileyonlinelibrary.com](http://wileyonlinelibrary.com)]



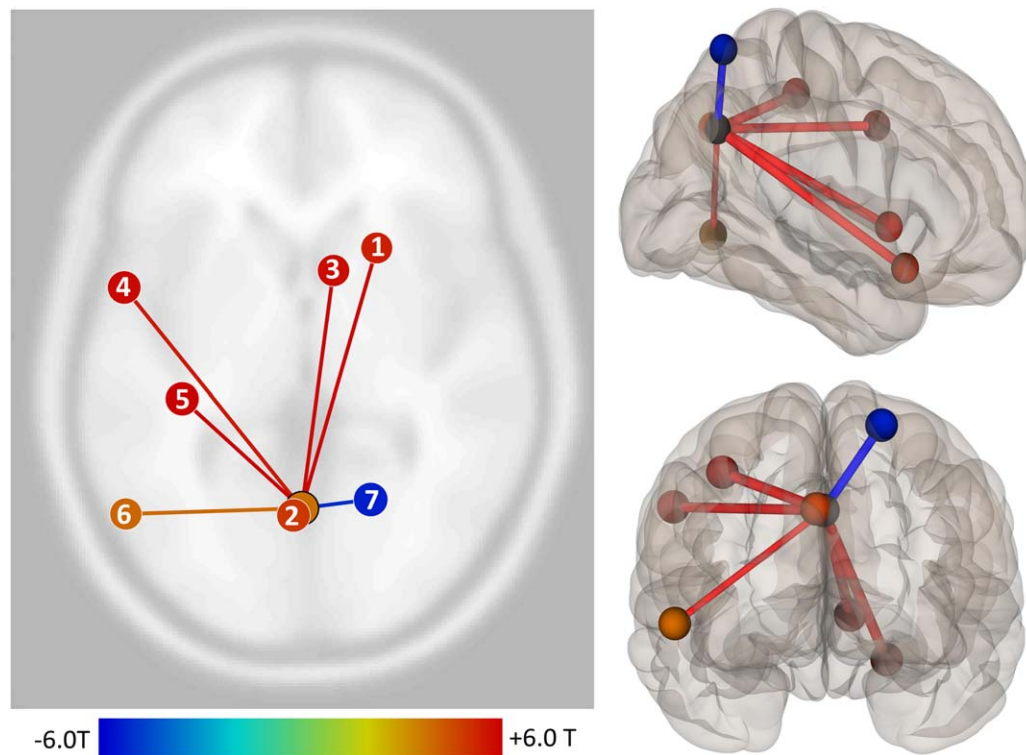


**FIGURE 3** Cortical and subcortical regions contributing to working memory load-associated degree centrality group differences at 6 weeks relative to presurgical baseline in the dorsal posterior cingulate cortex. *Note.* Regions contributing to the significant working memory load-associated group  $\times$  time task-based intrinsic connectivity contrast (ICC) degree centrality finding in the dPCC. (a) Right inferior frontal gyrus (MNI +22, +16, -20). (b) Left dorsal posterior cingulate cortex/precuneus region (MNI -2, -66, +34). (c) Right caudate nucleus (MNI +10, +14, 0). (d) Left superior frontal gyrus (MNI -56, +4, +36). (e) Left postcentral gyrus (MNI -38, -30, +50). (f) Left inferior temporal gyrus (-56, -68, -6). (g) Right superior parietal lobule (MNI +20, -62, +66); see Table 4. ICC contributor regions were determined via post-hoc seed-to-voxel analysis using dPCC seed from omnibus group  $\times$  time analysis of working memory load task-based ICC differences, adjusted for sex, perioperative global white matter hyperintensity volume change, and N-back performance accuracy change; omnibus analysis statistical thresholds apply (Table 3) [Color figure can be viewed at [wileyonlinelibrary.com](http://wileyonlinelibrary.com)]

in the right superior parietal lobule. This region was most strongly associated with working memory ( $r = 0.17$ , meta-analytic coactivation,  $r = 0.22$ ) and anticorrelated with the default mode search term ( $r = -0.24$ , meta-analytic coactivation,  $r = -0.06$ ).

### 3.10 | Post-hoc examination of neuroimaging, performance, and cognitive outcome data

#### 3.10.1 | Association of task-based FC change and perioperative N-back performance change

Post-hoc linear regression analyses were conducted to examine for relationships between regions that displayed significant 6 week postoperative degree centrality (ICC) and local coherence (ILC) changes and changes in in-scanner N-back task accuracy. Normalized  $z$  values denoting change in degree centrality for each ICC locus (6 weeks minus baseline) were extracted and plotted against the 6 weeks minus baseline change in 1-back and 2-back task accuracy. There were no statistically significant relationships between baseline to 6 week change in dPCC ICC and 1-back task accuracy change (e.g., surgery  $R^2 = 0.08$ ,  $p = .16$ , control  $R^2 = 0.00$ ,  $p = .85$ ) or with 2-back task accuracy change (e.g., surgery  $R^2 = 0.10$ ,  $p = .12$ , control  $R^2 = 0.13$ ,  $p = .07$ ).

#### 3.10.2 | Relationship of task-based FC change and perioperative global cognitive change

An inverse relationship was observed in surgical patients between increases in dPCC ICC change associated with working memory load from before to 6 weeks after surgery and decreased mean global cognitive performance over the same period [ $R^2 = 0.43$ ,  $\beta = -1.04$ ,  $T(23) = -4.13$ ,  $p < .001$ ; Figure 2D]. In contrast, no relationship was observed for ICC change in this region and mean global cognitive change in the control participants ( $R^2 < 0.001$ ,  $p = .96$ ). Similar to the finding of an inverse relationship between working memory load-related degree centrality (ICC) change in the dPCC and global cognitive change, there was a statistically significant inverse relationship between local coherence (ILC) in the dPCC (Table 3) and global cognitive changes in the surgery group [ $R^2 = 0.31$ ,  $\beta = -0.43$ ,  $T(23) = -3.18$ ,  $p = .004$ ], but not in nonsurgical controls ( $R^2 = 0.04$ ,  $p = .34$ ).

## 4 | DISCUSSION

Following cardiac surgery in older adults, we found task-based increases in working memory load-associated degree centrality and



local coherence in the dorsal posterior cingulate cortex (dPCC). The posterior cingulate cortex (PCC) is an important hub of the default mode network (DMN) and has been associated functions including long-term memory retrieval, attention, introspection, and arousal (Braga and Leech, 2015; Braga, Sharp, Leeson, Wise, & Leech, 2013; Leech, Braga, & Sharp, 2012). Additionally, the dPCC has been implicated as a possible common hub shared between the DMN and other large scale brain networks, assisting in resource allocation and outcomes during task performance (Pearson, Heilbronner, Barack, Hayden, & Platt, 2011) and modulating engagement as function of attentional focus (Leech et al., 2012; Utevsky, Smith, & Huettel, 2014). The involvement of DMN-associated regions during cognitive task performance runs counter to the conception of this "task negative" network being uninvolvement during concerted cognitive tasks (Spreng, 2012), but recent studies suggest that certain DMN regions modulate their connectivity in response to working memory performance demands (Esposito et al., 2009; Hampson et al., 2006; Spreng et al., 2014). These studies have revealed dynamic interactions between the DMN-associated angular gyri, dPCC, and frontoparietal network (FPN) regions a function of working memory performance and working memory load (Piccoli et al., 2015; Vatansever et al., 2016). Leech et al. (2012) found that the dPCC and ventral PCC (vPCC) fractionate respectively between FPN and DMN task-based functional connectivity during high cognitive demands, and it was the dPCC that deactivated strongest in association with an attentionally demanding cognitive task. Additionally, dPCC connectivity appears to be greater with attentional networks at rest, suggesting that this PCC subregion may be critical to internal/external switching of attentional focus between the DMN and FPN (Leech, Kamourieh, Beckmann, & Sharp, 2011; Leech et al., 2012). Alteration in DMN-associated PCC functional connectivity during working memory task performance has been described in various patient populations, including older adults with mild cognitive impairment (Kochan et al., 2010; Wang, Li, Yu, Huang, & Li, 2016), traumatic brain injury (van der Horn et al., 2015), cerebrovascular disease (Papma et al., 2012), and psychiatric conditions (Bedard et al., 2014; Oflaz et al., 2014). Additionally, individuals without objective cognitive test deficits who nonetheless complained of cognitive problems, exhibited greater functional activity within the DMN-associated PCC and FPN-associated precuneus regions during increased working memory demands (Dumas et al., 2013).

An examination of the regions accounting for our finding of postoperative degree centrality changes in the dPCC relative to controls appears to support the contention that the dPCC acts as a possible modulator hub for DMN and task-based network (FPN) interconnectivity. Relative to non-surgical controls and presurgical baseline, cardiac surgical patients demonstrated increased task-based functional connectivity of the dPCC to cortical and subcortical regions implicated in transient updating processes during working memory performance (e.g., inferior temporal gyrus, precentral gyrus, and caudate), while others have been consistently associated with sustained task engagement and maintenance (e.g., inferior frontal gyrus; Cohen et al., 1997; see Table 4 and Figure 3). The one region that showed a decrease in functional connectivity to the dPCC (e.g., superior parietal lobule) has been

traditionally associated with the FPN maintenance component of working memory (Wendelken, Bunge, & Carter, 2008). Consistent with Leech et al. (2012), the functional decoupling of the dPCC from this FPN region was observed under high task demand. Observed increases in local coherence of the dPCC during high task demand additionally reinforce the importance of this DMN subregion to attentional resource allocation. Furthermore, the magnitude of working memory load-associated degree centrality and the local coherence changes in the dPCC in cardiac surgery patients were inversely associated with postoperative global cognitive change (Figure 2D). This finding may reflect core difficulties in the efficient coordination of resources in functional brain networks governing directed cognitive processes in those surgery patients with the worst cognitive outcomes. The finding of increased task-related degree centrality and local coherence within the dPCC during high working memory load in our surgery patients was observed despite no appreciable differences in N-back task performance accuracy between groups or over time. The apparent lack of a relationship between the observed dPCC functional connectivity changes and N-back performances between groups raises the possibility that the observed dPCC changes reflect greater cognitive effort in patients relative to controls to affect the same level of working memory task performance. Conversely, the increases could be related to perceived cognitive problems in the surgical patients, as Dumas et al. (2013) previously found greater working memory load-related engagement of DMN and FPN-associated regions in individuals complaining of cognitive problems, yet without objective evidence of deficit. Unfortunately, we did not assess participants for their subjective experiences during *n*-back task performance, so it is difficult to know if there were significant differences in perceived cognitive effort to perform the *n*-back task relative to individuals' presurgical baseline.

We found no association between total perioperative FLAIR lesion volume changes and working memory load-associated FC changes. We did not perform transcranial Doppler ultrasound measurements, so we cannot perform the same analysis correlating intraoperative embolic load with postoperative fMRI activation changes as in the Abu-Omar et al. (2006) study. Limited prior research has suggested that cerebral small vessel disease may be associated with impaired DMN deactivation during working memory performances in patients with coincident mild cognitive impairment, but that finding was for a locus more centrally located within the posterior cingulate gyrus (i.e., anterior and inferior to our dPCC loci; Papma et al., 2012). Yet, it is possible that the global FLAIR lesion volume metric employed in the current study may be either insensitive to or under-estimate the impact of perioperative cerebrovascular damage on brain functional networks. Evidence from neuroimaging studies conducted during the acute in-hospital recovery phase (i.e., day 2–7) after open and transcatheter cardiac surgery indicate the presence of significant increases in emboli-related diffusion-weighted imaging (DWI) lesion volumes (Abdul-Jawad Altisent et al., 2016). The majority of these DWI-detected lesions resolve and are not visible on standard FLAIR scans beyond the acute recovery period (e.g., 4–6 weeks after surgery). While these acute DWI detected lesions may no longer visible beyond in-hospital recovery periods, it cannot be said that they do not have a longer lasting impact on cognition given recent

clinical trial evidence showing a strong correlation between acute DWI lesion volume and cognition 30 days after surgery (Kapadia et al., 2016).

Additional considerations that could account for our observed changes in postoperative cognition and task-based functional connectivity include delirium or changes in medications with known cognitive side-effects taken by surgical patients. Indeed, postoperative delirium has been associated with POCD and longer term changes in cognition (Deiner and Silverstein, 2009; Inouye et al., 2016), and anticholinergic medications have been associated with perioperative changes in cognition and delirium risk (Boustani et al., 2008; Han et al., 2001). However, none of the cardiac surgical patients in this study tested positive for delirium, arguing against delirium as a possible contributor to the cognitive dysfunction and functional connectivity changes reported here. Furthermore, there were no significant differences in anticholinergic medication frequencies between groups, over time or in their interaction, arguing against anticholinergic medication as a significant contributor to the postoperative cognitive and task-based functional connectivity changes observed in this study.

The postoperative task-based functional connectivity changes observed in this study could also be due to neuroinflammation. Surgery causes significant peripheral inflammatory and central neuroinflammatory responses (Vacas et al., 2013). In particular, cardiac surgery is known to produce >12-fold increases in cerebrospinal fluid (CSF) IL-6 levels, and a >4-fold increase in IL-8 levels (Reinsfelt, Westerlind, Blennow, Zetterberg, & Ricksten, 2013). Outside of the perioperative setting, neuroinflammation is known to cause changes in large-scale functional network connectivity (Labrenz et al., 2016), suggesting that the central neuroinflammatory response that is known to follow cardiac surgery could be sufficient to cause the connectivity changes reported in this paper. Due to high-dose anticoagulant therapy prior to cardiopulmonary bypass, we were unable to safely obtain perioperative cerebrospinal fluid neuroinflammatory biomarker data to directly test this possibility. However, our research team is currently investigating this possible systemic POCD mechanism on postsurgical functional connectivity and cognition in older adult noncardiac surgery patients.

The primary limitation of this study is its small sample size (25 cardiac surgery patients and 26 controls). However, our study sample is similar to those of other studies that have examined functional connectivity changes in anesthetized patients (Palanca et al., 2015; Purdon et al., 2013), and our study benefits from a prospective, longitudinal design. Nevertheless, our working memory load task-based functional connectivity differences between groups should be interpreted with caution until larger studies with more extended longitudinal follow-up can be conducted to confirm our findings. Our data are merely *correlative*, and cannot answer the question of whether altered DMN and FPN network modulation plays a *causal* role in cognitive dysfunction following cardiac surgery. Determining whether altered DMN modulation causes cognitive dysfunction following cardiac surgery may require neuromodulatory techniques to determine whether normalizing DMN regulation helps improve cognitive function after cardiac surgery, and/or whether altering DMN connectivity in nonsurgical patients is sufficient to replicate the cognitive dysfunction associated with POCD (in

the absence of surgery). Additionally, while all study analyses controlled for sex, our participant groups were not prospectively matched on sex; a limitation largely associated with recruitment challenges involving cardiac control and surgery participants with multiple exclusionary factors. Last, our observed task-based changes in degree centrality and local coherence of the dPCC may be specific only to working memory or high cognitive load tasks. It remains to be seen if there are alternative task-based functional connectivity changes after surgery specific to other cognitive functions (e.g., episodic memory).

We previously reported that the magnitude of cognitive dysfunction after cardiac surgery is positively associated with changes in degree centrality of the vPCC and right superior frontal gyrus during resting-state (Browndyke et al., 2017), and with this current investigation, we find working memory task-related changes in degree centrality and local coherence in dPCC DMN-associated areas that are also associated with postoperative cognitive outcomes. Taken together, our prior and present results strengthen the evidence that postoperative changes in functional connectivity characteristics during rest and task engagement in important midline posterior brain regions whose functional connectivity may be preferentially impacted by systemic neuroinflammation (Labrenz et al., 2016) and are sensitive to age-related neuropathological decline (Yu et al., 2017).

## ACKNOWLEDGMENTS

The authors thank our research associates: Yanne Toulgoat-Dubois, Rachele Brassard, and Kathryn Odom, and technical staff at the Duke Brain Imaging and Analysis Center (BIAC): Susan Music, Luther Pool, and Natalie Goutkin. They also thank Dr Simon Davis and Mathew Stanley and the members of the Cabeza Lab for their suggestions and comments on this article.

## CONFLICTS OF INTEREST

All the authors declare that they have no conflicts of interest with the contents of this article.

## ORCID

Jeffrey N. Browndyke  <http://orcid.org/0000-0002-8573-7073>

## REFERENCES

- Abdul-Jawad Altisent, O., Ferreira-Gonzalez, I., Marsal, J. R., Ribera, A., Auger, C., Ortega, G., ... Garcia-Dorado, D. (2016). Neurological damage after transcatheter aortic valve implantation compared with surgical aortic valve replacement in intermediate risk patients. *Clinical Research in Cardiology*, 105, 508–517.
- Abu-Omar, Y., Cader, S., Guerrieri Wolf, L., Pigott, D., Matthews, P. M., & Taggart, D. P. (2006). Short-term changes in cerebral activity in on-pump and off-pump cardiac surgery defined by functional magnetic resonance imaging and their relationship to microembolization. *Journal of Thoracic and Cardiovascular Surgery*, 132, 1119–1125.
- Anticevic, A., Cole, M. W., Murray, J. D., Corlett, P. R., Wang, X. J., & Krystal, J. H. (2012). The role of default network deactivation in cognition and disease. *Trends in Cognitive Sciences*, 16, 584–592.

- Bedard, A. C., Newcorn, J. H., Clerkin, S. M., Krone, B., Fan, J., Halperin, J. M., & Schulz, K. P. (2014). Reduced prefrontal efficiency for visuo-spatial working memory in attention-deficit/hyperactivity disorder. *Journal of the American Academy of Child and Adolescent Psychiatry*, 53, 1020–1030 e6.
- Behzadi, Y., Restom, K., Liau, J., & Liu, T. T. (2007). A component based noise correction method (CompCor) for BOLD and perfusion based fMRI. *NeuroImage*, 37, 90–101.
- Berger, M., Burke, J., Eckenhoof, R., & Mathew, J. (2014). Alzheimer's disease, anesthesia, and surgery: A clinically focused review. *Journal of Cardiothoracic and Vascular Anesthesia*, 28, 1609–1623.
- Berger, M., Nadler, J. W., Browndyke, J., Terrando, N., Ponnusamy, V., Cohen, H. J., ... Mathew, J. P. (2015). Postoperative cognitive dysfunction: Minding the gaps in our knowledge of a common postoperative complication in the elderly. *Anesthesiology Clinics*, 33, 517–550.
- Boustani, M. A., Campbell, N., Munger, S., Maidment, I. D., & Fox, C. (2008). Impact of anticholinergics on the aging brain: A review and practical application. *Aging Health*, 4, 311–320.
- Braga, R. M., & Leech, R. (2015). Echoes of the brain: Local-scale representation of whole-brain functional networks within transmodal cortex. *Neuroscientist*.
- Braga, R. M., Sharp, D. J., Leeson, C., Wise, R. J., & Leech, R. (2013). Echoes of the brain within default mode, association, and heteromodal cortices. *The Journal of Neuroscience: The Official Journal of the Society for Neuroscience*, 33, 14031–14039.
- Braunlich, K., Gomez-Lavin, J., & Seger, C. A. (2015). Frontoparietal networks involved in categorization and item working memory. *NeuroImage*, 107, 146–162.
- Brown, W. R., Moody, D. M., Challa, V. R., Stump, D. A., & Hammon, J. W. (2000). Longer duration of cardiopulmonary bypass is associated with greater numbers of cerebral microemboli. *Stroke*, 31, 707–713.
- Browndyke, J. N., Berger, M., Harshbarger, T. B., Smith, P. J., White, W., Bisanar, T. L., ... Mathew, J. P. (2017). Resting-state functional connectivity and cognition after major cardiac surgery in older adults without preoperative cognitive impairment: Preliminary findings. *Journal of the American Geriatrics Society*, 65, e6–e12.
- Browndyke, J. N., Moser, D. J., Cohen, R. A., O'Brien, D. J., Algina, J. J., Haynes, W. G., ... Bauer, R. M. (2002). Acute neuropsychological functioning following cardiosurgical interventions associated with the production of intraoperative cerebral microemboli. *Clinical Neuropsychology*, 16, 463–471.
- Campbell, N., Perkins, A., Hui, S., Khan, B., & Boustani, M. (2011). Association between prescribing of anticholinergic medications and incident delirium: A cohort study. *Journal of the American Geriatrics Society*, 59 (Suppl 2), S277–S281.
- Canet, J., Raeder, J., Rasmussen, L. S., Enlund, M., Kuipers, H. M., Hanning, C. D., ... Investigators, I. (2003). Cognitive dysfunction after minor surgery in the elderly. *Acta Anaesthesiologica Scandinavica*, 47, 1204–1210.
- Casaleto, K. B., Cattie, J., Franklin, D. R., Moore, D. J., Woods, S. P., Grant, I., ... Group, H. (2014). The Wide Range Achievement Test-4 Reading subtest "holds" in HIV-infected individuals. *Journal of Clinical and Experimental Neuropsychology*, 36, 992–1001.
- Cerejeira, J., Firmino, H., Vaz-Serra, A., & Mukaetova-Ladinska, E. B. (2010). The neuroinflammatory hypothesis of delirium. *Acta Neuropathologica*, 119, 737–754.
- Coburn, M., Fahlenkamp, A., Zoremba, N., & Schaelte, G. (2010). Postoperative cognitive dysfunction: Incidence and prophylaxis. *Der Anaesthesist*, 59, 177–184. quiz 185.
- Cockrell, J. R., & Folstein, M. F. (1988). Mini-Mental State Examination (MMSE). *Psychopharmacology Bulletin*, 24, 689–692.
- Cohen, J. D., Perlstein, W. M., Braver, T. S., Nystrom, L. E., Noll, D. C., Jonides, J., & Smith, E. E. (1997). Temporal dynamics of brain activation during a working memory task. *Nature*, 386, 604–608.
- Collette, F., & Van der Linden, M. (2002). Brain imaging of the central executive component of working memory. *Neuroscience & Biobehavioral Reviews*, 26, 105–125.
- Constable, R. T., Vohr, B. R., Scheinost, D., Benjamin, J. R., Fulbright, R. K., Lacadie, C., ... Ment, L. R. (2013). A left cerebellar pathway mediates language in prematurely-born young adults. *NeuroImage*, 64, 371–378.
- Cook, D. J., Huston, J., 3rd, Trenerry, M. R., Brown, R. D., Jr., Zehr, K. J., & Sundt, T. M. 3rd. (2007). Postcardiac surgical cognitive impairment in the aged using diffusion-weighted magnetic resonance imaging. *The Annals of Thoracic Surgery*, 83, 1389–1395.
- Cortese, G. P., & Burger, C. (2017). Neuroinflammatory challenges compromise neuronal function in the aging brain: Postoperative cognitive delirium and Alzheimer's disease. *Behavioural Brain Research*, 322, 269–279.
- D'Esposito, M. (2007). From cognitive to neural models of working memory. *Philosophical Transactions of the Royal Society of London. Series B Biological Sciences*, 362, 761–772.
- Deiner, S., & Silverstein, J. H. (2009). Postoperative delirium and cognitive dysfunction. *British Journal of Anaesthesia*, 103(Suppl 1), i41–i46.
- Deshpande, G., Keressens, C., Sebel, P. S., & Hu, X. (2010). Altered local coherence in the default mode network due to sevoflurane anesthesia. *Brain Research*, 1318, 110–121.
- Deshpande, G., LaConte, S., Peltier, S., & Hu, X. (2009). Integrated local correlation: A new measure of local coherence in fMRI data. *Human Brain Mapping*, 30, 13–23.
- Di Napoli, M., & Shah, I. M. (2011). Neuroinflammation and cerebrovascular disease in old age: A translational medicine perspective. *Journal of Aging Research*, 2011, 857484.
- Duff, K. (2012). Evidence-based indicators of neuropsychological change in the individual patient: Relevant concepts and methods. *Archives of Clinical Neuropsychology*, 27, 248–261.
- Dumas, J. A., Kutz, A. M., McDonald, B. C., Naylor, M. R., Pfaff, A. C., Saykin, A. J., & Newhouse, P. A. (2013). Increased working memory-related brain activity in middle-aged women with cognitive complaints. *Neurobiology of Aging*, 34, 1145–1147.
- Ekman, M., Fiebach, C. J., Melzer, C., Tittgemeyer, M., & Derrfuss, J. (2016). Different roles of direct and indirect frontoparietal pathways for individual working memory capacity. *Journal of Neuroscience*, 36, 2894–2903.
- Ely, E. W., Margolin, R., Francis, J., May, L., Truman, B., Dittus, R., ... Inouye, S. K. (2001). Evaluation of delirium in critically ill patients: Validation of the Confusion Assessment Method for the Intensive Care Unit (CAM-ICU). *Critical Care Medicine*, 29, 1370–1379.
- Esposito, F., Aragri, A., Latorre, V., Popolizio, T., Scarabino, T., Cirillo, S., ... Di Salle, F. (2009). Does the default-mode functional connectivity of the brain correlate with working-memory performances? *Archives Italiennes de Biologie*, 147, 11–20.
- Fox, C., Richardson, K., Maidment, I. D., Savva, G. M., Matthews, F. E., Smithard, D., ... Brayne, C. (2011). Anticholinergic medication use and cognitive impairment in the older population: The medical research council cognitive function and ageing study. *Journal of the American Geriatrics Society*, 59, 1477–1483.
- Gao, L., Taha, R., Gauvin, D., Othmen, L. B., Wang, Y., & Blaise, G. (2005). Postoperative cognitive dysfunction after cardiac surgery. *Chest*, 128, 3664–3670.
- Guo, W., Liu, F., Yu, M., Zhang, J., Zhang, Z., Liu, J., ... Zhao, J. (2015). Decreased regional activity and network homogeneity of the fronto-

- limbic network at rest in drug-naïve major depressive disorder. *Australian & New Zealand Journal of Psychiatry*, 49, 550–556.
- Hampson, M., Driesen, N. R., Skudlarski, P., Gore, J. C., & Constable, R. T. (2006). Brain connectivity related to working memory performance. *The Journal of Neuroscience: The Official Journal of the Society for Neuroscience*, 26, 13338–13343.
- Han, L., McCusker, J., Cole, M., Abrahamowicz, M., Primeau, F., & Elie, M. (2001). Use of medications with anticholinergic effect predicts clinical severity of delirium symptoms in older medical inpatients. *Archives of Internal Medicine*, 161, 1099–1105.
- Henson, R. N. (2015). Analysis of variance (ANOVA). In A.W. Toga (Ed.), *Brain mapping: An encyclopedic reference* (pp. 477–481). Academic Press.
- Henson, R. N. A., & Penny, W. D. (2005). *ANOVAs and SPM: Technical report*. Wellcome Department of Imaging Neuroscience.
- Hirsch, J., Vacas, S., Terrando, N., Yuan, M., Sands, L. P., Kramer, J., ... Leung, J. M. (2016). Perioperative cerebrospinal fluid and plasma inflammatory markers after orthopedic surgery. *Journal of Neuroinflammation*, 13, 211.
- Hovens, I. B., van Leeuwen, B. L., Mariani, M. A., Kraneveld, A. D., & Schoemaker, R. G. (2016). Postoperative cognitive dysfunction and neuroinflammation; Cardiac surgery and abdominal surgery are not the same. *Brain, Behavior, and Immunity*, 54, 178–193.
- Ida, M., & Kawaguchi, M. (2014). Postoperative cognitive dysfunction after non-cardiac surgery. *Masui. The Japanese Journal of Anesthesiology*, 63, 1228–1234.
- Inouye, S. K., Marcantonio, E. R., Kosar, C. M., Tommet, D., Schmitt, E. M., Trivison, T. G., ... Jones, R. N. (2016). The short-term and long-term relationship between delirium and cognitive trajectory in older surgical patients. *Alzheimers Dementia*, 12, 766–775.
- Johnson, T., Monk, T., Rasmussen, L. S., Abildstrom, H., Houx, P., Korttila, K., ... Investigators, I. (2002). Postoperative cognitive dysfunction in middle-aged patients. *Anesthesiology*, 96, 1351–1357.
- Kapadia, S. R., Kodali, S., Makkar, R., Mehran, R., Lazar, R. M., Zivadinov, R., ... Linke, A. (2016). Cerebral embolic protection during transcatheter aortic valve replacement. *Journal of the American College of Cardiology*.
- Kearney-Ramos, T. E., Fausett, J. S., Gess, J. L., Reno, A., Peraza, J., Kilts, C. D., & James, G. A. (2014). Merging clinical neuropsychology and functional neuroimaging to evaluate the construct validity and neural network engagement of the n-back task. *Journal of the International Neuropsychological Society*, 20, 736–750.
- Kochan, N. A., Breakspear, M., Slavin, M. J., Valenzuela, M., McCraw, S., Brodaty, H., & Sachdev, P. S. (2010). Functional alterations in brain activation and deactivation in mild cognitive impairment in response to a graded working memory challenge. *Dementia and Geriatric Cognitive Disorders*, 30, 553–568.
- Kotekar, N., Kuruvilla, C. S., & Murthy, V. (2014). Post-operative cognitive dysfunction in the elderly: A prospective clinical study. *Indian Journal of Anaesthesia*, 58, 263–268.
- Kruijs, R. W., Vlasveld, F. A., & Van Dijk, D. (2010). The (un)importance of cerebral microemboli. *Seminars in Cardiothoracic and Vascular Anesthesia*, 14, 111–118.
- Labrenz, F., Wrede, K., Forsting, M., Engler, H., Schedlowski, M., Elsenbruch, S., & Benson, S. (2016). Alterations in functional connectivity of resting state networks during experimental endotoxemia - An exploratory study in healthy men. *Brain, Behavior, and Immunity*, 54, 17–26.
- Lancaster, J. L., Woldorff, M. G., Parsons, L. M., Liotti, M., Freitas, C. S., Rainey, L., ... Fox, P. T. (2000). Automated Talairach atlas labels for functional brain mapping. *Human Brain Mapping*, 10, 120–131.
- Lee, H. W., Arora, J., Papademetris, X., Tokoglu, F., Negishi, M., Scheinost, D., ... Constable, R. T. (2014). Altered functional connectivity in seizure onset zones revealed by fMRI intrinsic connectivity. *Neurology*, 83, 2269–2277.
- Leech, R., Braga, R., & Sharp, D. J. (2012). Echoes of the brain within the posterior cingulate cortex. *The Journal of Neuroscience: The Official Journal of the Society for Neuroscience*, 32, 215–222.
- Leech, R., Kamourieh, S., Beckmann, C. F., & Sharp, D. J. (2011). Fractionating the default mode network: Distinct contributions of the ventral and dorsal posterior cingulate cortex to cognitive control. *Journal of Neuroscience*, 31, 3217–3224.
- Lewinsohn, P. M., Seeley, J. R., Roberts, R. E., & Allen, N. B. (1997). Center for Epidemiologic Studies Depression Scale (CES-D) as a screening instrument for depression among community-residing older adults. *Psychology and Aging*, 12, 277–287.
- Liang, X., Zou, Q., He, Y., & Yang, Y. (2016). Topologically reorganized connectivity architecture of default-mode, executive-control, and salience networks across working memory task loads. *Cerebral Cortex*, 26, 1501–1511.
- Liu, H., Liu, Z., Liang, M., Hao, Y., Tan, L., Kuang, F., ... Jiang, T. (2006). Decreased regional homogeneity in schizophrenia: A resting state functional magnetic resonance imaging study. *Neuroreport*, 17, 19–22.
- Liu, Y. H., Wang, D. X., Li, L. H., Wu, X. M., Shan, G. J., Su, Y., ... Sun, W. (2009). The effects of cardiopulmonary bypass on the number of cerebral microemboli and the incidence of cognitive dysfunction after coronary artery bypass graft surgery. *Anesthesia & Analgesia*, 109, 1013–1022.
- Lombard, F. W., & Mathew, J. P. (2010). Neurocognitive dysfunction following cardiac surgery. *Seminars in Cardiothoracic and Vascular Anesthesia*, 14, 102–110.
- Lynch, J. E., & Riley, J. B. (2008). Microemboli detection on extracorporeal bypass circuits. *Perfusion*, 23, 23–32.
- Maddahi, A., & Edvinsson, L. (2010). Cerebral ischemia induces microvascular pro-inflammatory cytokine expression via the MEK/ERK pathway. *Journal of Neuroinflammation*, 7, 14.
- Martuzzi, R., Ramani, R., Qiu, M., Shen, X., Papademetris, X., & Constable, R. T. (2011). A whole-brain voxel based measure of intrinsic connectivity contrast reveals local changes in tissue connectivity with anesthetic without a priori assumptions on thresholds or regions of interest. *NeuroImage*, 58, 1044–1050.
- Mathew, J. P., White, W. D., Schinderle, D. B., Podgoreanu, M. V., Berger, M., Milano, C. A., ... Neurologic Outcome Research Group Of The Duke Heart, C. (2013). Intraoperative magnesium administration does not improve neurocognitive function after cardiac surgery. *Stroke*, 44, 3407–3413.
- McDonagh, D. L., Mathew, J. P., White, W. D., Phillips-Bute, B., Laskowitz, D. T., Podgoreanu, M. V., & Newman, M. F. Neurologic Outcome Research, G. (2010). Cognitive function after major noncardiac surgery, apolipoprotein E4 genotype, and biomarkers of brain injury. *Anesthesiology*, 112, 852–859.
- Monk, T. G., Weldon, B. C., Garvan, C. W., Dede, D. E., van der Aa, M. T., Heilman, K. M., & Gravenstein, J. S. (2008). Predictors of cognitive dysfunction after major noncardiac surgery. *Anesthesiology*, 108, 18–30.
- Motallebzadeh, R., Bland, J. M., Markus, H. S., Kaski, J. C., & Jahangiri, M. (2007). Neurocognitive function and cerebral emboli: Randomized study of on-pump versus off-pump coronary artery bypass surgery. *The Annals of Thoracic Surgery*, 83, 475–482.
- Newfield, P. (2009). Postoperative cognitive dysfunction. *F1000 Med Rep*, 1.



- Newman, M. F., Grocott, H. P., Mathew, J. P., White, W. D., Landolfo, K., Reves, J. G., ... Duke Heart, C. (2001a). Report of the substudy assessing the impact of neurocognitive function on quality of life 5 years after cardiac surgery. *Stroke*, 32, 2874–2881.
- Newman, M. F., Kirchner, J. L., Phillips-Bute, B., Gaver, V., Grocott, H., Jones, R. H., ... Blumenthal, J. A. Neurological Outcome Research, G., the Cardiothoracic Anesthesiology Research Endeavors, I. (2001b). Longitudinal assessment of neurocognitive function after coronary-artery bypass surgery. *The New England Journal of Medicine*, 344, 395–402.
- Newman, S., Stygall, J., Hirani, S., Shaefi, S., & Maze, M. (2007). Postoperative cognitive dysfunction after noncardiac surgery: A systematic review. *Anesthesiology*, 106, 572–590.
- Notzold, A., Khattab, A. A., & Eggers, J. (2006). Microemboli in aortic valve replacement. *Expert Review of Cardiovascular Therapy*, 4, 853–859.
- Oflaz, S., Akyuz, F., Hamamci, A., Firat, Z., Kesinkilic, C., Kilickesmez, O., & Cihangiroglu, M. (2014). Working memory dysfunction in delusional disorders: An fMRI investigation. *Journal of Psychiatric Research*, 56, 43–49.
- Palanca, B. J., Mitra, A., Larson-Prior, L., Snyder, A. Z., Avidan, M. S., & Raichle, M. E. (2015). Resting-state functional magnetic resonance imaging correlates of sevoflurane-induced unconsciousness. *Anesthesiology*, 123, 346–356.
- Papma, J. M., den Heijer, T., de Koning, I., Mattace-Raso, F. U., van der Lugt, A., van der Lijn, F., ... Prins, N. D. (2012). The influence of cerebral small vessel disease on default mode network deactivation in mild cognitive impairment. *NeuroImage Clinics*, 2, 33–42.
- Patel, N., Minhas, J. S., & Chung, E. M. (2015). The presence of new MRI lesions and cognitive decline after cardiac surgery: A systematic review. *Journal of Cardiac Surgery*, 30, 808–812.
- Pearson, J. M., Heilbronner, S. R., Barack, D. L., Hayden, B. Y., & Platt, M. L. (2011). Posterior cingulate cortex: Adapting behavior to a changing world. *Trends in Cognitive Sciences*, 15, 143–151.
- Phillips-Bute, B., Mathew, J. P., Blumenthal, J. A., Grocott, H. P., Laskowitz, D. T., Jones, R. H., ... Newman, M. F. (2006). Association of neurocognitive function and quality of life 1 year after coronary artery bypass graft (CABG) surgery. *Psychosomatic Medicine*, 68, 369–375.
- Piccoli, T., Valente, G., Linden, D. E., Re, M., Esposito, F., Sack, A. T., & Salle, F. D. (2015). The default mode network and the working memory network are not anti-correlated during all phases of a working memory task. *PLoS One*, 10, e0123354.
- Price, C. C., Garvan, C. W., & Monk, T. G. (2008). Type and severity of cognitive decline in older adults after noncardiac surgery. *Anesthesiology*, 108, 8–17.
- Purdon, P. L., Pierce, E. T., Mukamel, E. A., Prerau, M. J., Walsh, J. L., Wong, K. F., ... Brown, E. N. (2013). Electroencephalogram signatures of loss and recovery of consciousness from propofol. *Proceedings of the National Academy of Sciences of the United States of America*, 110, E1142–E1151.
- Raja, P. V., Blumenthal, J. A., & Doraiswamy, P. M. (2004). Cognitive deficits following coronary artery bypass grafting: Prevalence, prognosis, and therapeutic strategies. *CNS Spectrums*, 9, 763–772.
- Ramaiah, R., & Lam, A. M. (2009). Postoperative cognitive dysfunction in the elderly. *Anesthesiology Clinics*, 27, 485–496, table of contents.
- Rappold, T., Laflam, A., Hori, D., Brown, C., Brandt, J., Mintz, C. D., ... Hogue, C. W. (2016). Evidence of an association between brain cellular injury and cognitive decline after non-cardiac surgery. *British Journal of Anaesthesia*, 116, 83–89.
- Rasmussen, L. S. (2006). Postoperative cognitive dysfunction: Incidence and prevention. Best practice & research. *Clinical Anaesthesiology*, 20, 315–330.
- Reinsfelt, B., Westerlind, A., Blennow, K., Zetterberg, H., & Ricksten, S. E. (2013). Open-heart surgery increases cerebrospinal fluid levels of Alzheimer-associated amyloid beta. *Acta Anaesthesiologica Scandinavica*, 57, 82–88.
- Reitan, R. M. (1958). Validity of the Trail Making test as an indicator of organic brain damage. *Perceptual and Motor Skills*, 8, 271–276.
- Rodriguez, R. A., Rubens, F. D., Wozny, D., & Nathan, H. J. (2010). Cerebral emboli detected by transcranial Doppler during cardiopulmonary bypass are not correlated with postoperative cognitive deficits. *Stroke*, 41, 2229–2235.
- Sauer, A. M., Kalkman, C., & van Dijk, D. (2009). Postoperative cognitive decline. *Journal of Anesthesia*, 23, 256–259.
- Sawrie, S. M., Chelune, G. J., Naugle, R. I., & Luders, H. O. (1996). Empirical methods for assessing meaningful neuropsychological change following epilepsy surgery. *Journal of the International Neuropsychological Society*, 2, 556–564.
- Scheinost, D., Benjamin, J., Lacadie, C. M., Vohr, B., Schneider, K. C., Ment, L. R., ... Constable, R. T. (2012). The intrinsic connectivity distribution: A novel contrast measure reflecting voxel level functional connectivity. *NeuroImage*, 62, 1510–1519.
- Schlosser, R. G., Wagner, G., & Sauer, H. (2006). Assessing the working memory network: Studies with functional magnetic resonance imaging and structural equation modeling. *Neuroscience*, 139, 91–103.
- Schmidt, M. (1996). *Rey auditory and verbal learning test: A handbook*. Los Angeles, CA: Western Psychological Services.
- Schmidt, P., Gaser, C., Arsic, M., Buck, D., Forschler, A., Berthele, A., ... Muhlau, M. (2012). An automated tool for detection of FLAIR-hyperintense white-matter lesions in multiple sclerosis. *NeuroImage*, 59, 3774–3783.
- Scott, D. A., Evered, L. A., Gerraty, R. P., MacIsaac, A., Lai-Kwon, J., & Silbert, B. S. (2014). Cognitive dysfunction follows left heart catheterisation but is not related to microembolic count. *International Journal of Cardiology*, 175, 67–71.
- Sessler, C. N., Gosnell, M. S., Grap, M. J., Brophy, G. M., O'neal, P. V., Keane, K. A., ... Elswick, R. K. (2002). The Richmond Agitation-Sedation Scale: Validity. *American Journal of Respiratory and Critical Care Medicine*, 166, 1338–1344.
- Silvis, J. D., Belopolsky, A. V., Murris, J. W., & Donk, M. (2015). The effects of feature-based priming and visual working memory on oculomotor capture. *PLoS One*, 10, e0142666.
- Spreng, R. N. (2012). The fallacy of a “task-negative” network. *Frontiers in Psychology*, 3, 145.
- Spreng, R. N., DuPre, E., Selarka, D., Garcia, J., Gojkovic, S., Mildner, J., ... Turner, G. R. (2014). Goal-congruent default network activity facilitates cognitive control. *Journal of Neuroscience*, 34, 14108–14114.
- Stanley, M. L., Dagenbach, D., Lyday, R. G., Burdette, J. H., & Laurienti, P. J. (2014). Changes in global and regional modularity associated with increasing working memory load. *Frontiers in Human Neuroscience*, 8, 954.
- Tomasi, D., & Volkow, N. D. (2010). Functional connectivity density mapping. *Proceedings of the National Academy of Sciences of the United States of America*, 107, 9885–9890.
- Trites, R. (2002). *Grooved pegboard test: User instructions*. Lafayette, IN: Lafayette Instrument Company.
- Utevsky, A. V., Smith, D. V., & Huettel, S. A. (2014). Precuneus is a functional core of the default-mode network. *The Journal of Neuroscience: The Official Journal of the Society for Neuroscience*, 34, 932–940.
- Vacas, S., Degos, V., Feng, X., & Maze, M. (2013). The neuroinflammatory response of postoperative cognitive decline. *British Medical Bulletin*, 106, 161–178.



- van der Horn, H. J., Liemburg, E. J., Scheenen, M. E., de Koning, M. E., Spikman, J. M., & van der Naalt, J. (2015). Post-concussive complaints after mild traumatic brain injury associated with altered brain networks during working memory performance. *Brain Imaging and Behavior*, 10, 1243–1253.
- van Dijk, D., Dieleman, J. M., & Hijman, R. (2007). Postoperative cognitive dysfunction. *Nederlands Tijdschrift Voor Geneeskunde*, 151, 1163–1166.
- Vatansever, D., Manktelow, A. E., Sahakian, B. J., Menon, D. K., & Stamatidis, E. A. (2016). Angular default mode network connectivity across working memory load. *Human Brain Mapping*, 38, 41–52.
- Wang, P., Li, R., Yu, J., Huang, Z., & Li, J. (2016). Frequency-dependent brain regional homogeneity alterations in patients with mild cognitive impairment during working memory state relative to resting state. *Frontiers in Aging Neuroscience*, 8, 60.
- Wechsler, D. (1987). *Wechsler memory scale-revised*. New York, NY: The Psychological Corporation.
- Wechsler, D. (1997). *Wechsler Adult Intelligence Scale—Third edition*. San Antonio, TX: The Psychological Corporation.
- Wendelken, C., Bunge, S. A., & Carter, C. S. (2008). Maintaining structured information: An investigation into functions of parietal and lateral prefrontal cortices. *Neuropsychologia*, 46, 665–678.
- Whitfield-Gabrieli, S., & Nieto-Castanon, A. (2012). Conn: A functional connectivity toolbox for correlated and anticorrelated brain networks. *Brain Connectivity*, 2, 125–141.
- Wilkinson, G. S., & Robertson, G. J. (2006). *Wide Range Achievement Test 4 (WRAT-4): Professional manual*. Lutz, FL: Psychological Assessment Resources.
- Woodward, T. S., Cairo, T. A., Ruff, C. C., Takane, Y., Hunter, M. A., & Ngan, E. T. (2006). Functional connectivity reveals load dependent neural systems underlying encoding and maintenance in verbal working memory. *Neuroscience*, 139, 317–325.
- Xu, J., Calhoun, V. D., Pearson, G. D., & Potenza, M. N. (2014). Opposite modulation of brain functional networks implicated at low vs. high demand of attention and working memory. *PLoS One*, 9, e87078.
- Yarkoni, T., Poldrack, R. A., Nichols, T. E., Van Essen, D. C., & Wager, T. D. (2011). Large-scale automated synthesis of human functional neuroimaging data. *Nature Methods*, 8, 665–670.
- Yassi, N., Malpas, C. B., Campbell, B. C., Moffat, B., Steward, C., Parsons, M. W., ... Bivard, A. (2015). Contralateral thalamic surface atrophy and functional disconnection 3 months after ischemic stroke. *Cerebrovascular Diseases*, 39, 232–241.
- Yu, E., Liao, Z., Mao, D., Zhang, Q., Ji, G., et al. (2017). Directed functional connectivity of posterior cingulate cortex and whole brain in Alzheimer's disease and mild cognitive impairment. *Curr Alzheimer Res.*, 14, 628–635.
- Zanatta, P., Forti, A., Minniti, G., Comin, A., Mazzarolo, A. P., Chilufya, M., ... Polesel, E. (2013). Brain emboli distribution and differentiation during cardiopulmonary bypass. *Journal of Cardiothoracic and Vascular Anesthesia*, 27, 865–875.
- Zang, Y., Jiang, T., Lu, Y., He, Y., & Tian, L. (2004). Regional homogeneity approach to fMRI data analysis. *NeuroImage*, 22, 394–400.
- Zhang, Z., Liu, Y., Jiang, T., Zhou, B., An, N., Dai, H., ... Zhang, X. (2012). Altered spontaneous activity in Alzheimer's disease and mild cognitive impairment revealed by regional homogeneity. *NeuroImage*, 59, 1429–1440.

## SUPPORTING INFORMATION

Additional Supporting Information may be found online in the supporting information tab for this article.

**How to cite this article:** Browndyke JN, Berger M, Smith PJ, et al. Task-related changes in degree centrality and local coherence of the posterior cingulate cortex after major cardiac surgery in older adults. *Hum Brain Mapp*. 2018;39:985–1003. <https://doi.org/10.1002/hbm.23898>

## APPENDIX : NEUROLOGIC OUTCOME RESEARCH GROUP

**Director:** Joseph P. Mathew, M.D.

**Co-Director:** James A. Blumenthal, Ph.D.

**Anesthesiology:** Narai Balajonda, M.D.; Miles Berger, M.D., Ph.D.; Tiffany Bisanar, R.N., B.S.N.; Rachele Brassard, B.S.W.; Mary Cooter, M.S.; Bonita L. Funk, R.N.; Jorn A. Karhausen, M.D.; Miklos D. Kertai, M.D.; Rebecca Y. Klinger, M.D., M.S.; Yi-Ju Li, Ph.D.; Joseph P. Mathew, M.D.; Mark F. Newman, M.D.; Mihai V. Podgoreanu, M.D.; Mark Stafford-Smith, M.D.; Madhav Swaminathan, M.D.; Niccolo Terrando, Ph.D.; Yanne Toulgoat-Dubois, B.A.; David S. Warner, M.D., CCRP; Peter Waweru, CCRP.

**Psychiatry & Behavioral Medicine:** Michael A. Babyak, Ph.D.; James A. Blumenthal, Ph.D.; Jeffrey N. Browndyke, Ph.D.; Patrick Smith, Ph.D.; Kathleen A. Welsh-Bohmer, Ph.D.

**Cardiology:** Michael H. Sketch, Jr., M.D.

**Neurology:** Ellen R. Bennett, Ph.D.; Carmelo Graffagnino, M.D.; Daniel T. Laskowitz, M.D.

**Perfusion Services:** Kevin Collins, B.S., C.C.P.; Greg Smigla, B.S., C.C.P.; Ian Shearer, B.S., C.C.P.

**Surgery:** Thomas A. D'Amico, M.D.; Mani A. Daneshmand, M.D.; R. Jeffrey G. Gaca, M.D.; Donald D. Glower, M.D.; Jack Haney, M.D.; R. David Harpole, M.D.; Mathew G. Hartwig, M.D.; G. Chad Hughes, M.D.; Jacob A. Klapper, M.D.; Shu S. Lin, M.D.; Andrew J. Lodge, M.D.; Carmelo A. Milano, M.D.; Ryan P. Plichta, M.D.; Jacob N. Schroeder, M.D.; Peter K. Smith, M.D.; Betty C. Tong, M.D.